Divecha Centre for Climate Change

Indian Institute of Science

Climate Change Reports

Studies on the Dynamics of Glaciers

T. N. Ventakesh, A. V. Kulkarni
and **J. Srinivasan**

REPORT IISc-DCCC 12 CC1 JUNE 2012

Divecha Centre for Climate Change

Indian Institute of Science

Climate Change Reports

Studies on the Dynamics of Glaciers

T. N. Ventakesh, A. V. Kulkarni
and **J. Srinivasan**

REPORT IISc-DCCC 12 CC1 JUNE 2012

Studies on the dynamics of glaciers

T. N. Venkatesh [1], A. V. Kulkarni and J. Srinivasan

tnv@flosolver.nal.res.in
anilkulkarni@caos.iisc.ernet.in
jayes@caos.iisc.ernet.in

June 2012

[1]CSIR-NAL, Bangalore

Contents

Acknowledgements

This work was done while the first author was on sabbatical at IISc. Bangalore during the period November 2010 – November 2011. Studies were carried out at the Divecha Centre for Climate change on the numerical modelling of glaciers and are documented in this report. The support of Director, CSIR-NAL Bangalore and colleagues at the Flosolver Unit, NAL is gratefully acknowledged.

Chapter 1

Introduction

Glaciers are "rivers of ice" which are present in the polar regions and high altitude mountain ranges. While there has been a wealth of observations, measurements and ideas about them since the 1700s, they have been objects of modern scientific study since the mid-twentieth century (Cuffey and Patterson, 2010). Of late, there has been an increased interest in the study and modelling of glaciers since they serve as markers of climate change (Oerlemans, 2005).

Figure 1.1: *A typical glacier in the Himalayas.*

.

In the Himalayas, while a majority of glaciers are retreating (Kulkarni et al., 2007), some are stationary and a few advancing. Scherler et al. (2011) used satellite imagery to assess the movement of a large number of glaciers in the Himalayas and found that

different responses in different regions, with advance in the Karakoram region and retreat in the other regions. They attribute this change in behavior to presence of debris cover. The accumulation of debris is linked to the slopes in the accumulation and terminus regions.

Figure 1.2: *The Samudra Tapu glacier.*

.

Dynamics of glaciers can be studied using analytical and numerical models. Analytical models with appropriate assumptions can provide insight into the overall behaviour (Oerlemans, 2008). Numerical models of varying sophistication are possible for studying glaciers. These can range from one-dimensional ice-flow models (Adhikari and Huybrechts, 2009), or more complex models (Kotlarski et al., 2010). Even simple models have been shown to be quite effective in simulating the observed data over the past fifty years.

In this report, the studies done on the dynamics of glaciers is documented. In chapter 2, derivation and method of solution of the one-dimensional ice-flow model is described. In chapter 3, the model problem chosen for understanding the role of slope in the basic dynamics is described. Our hypothesis on the relative effect of slope and equilibrium line altitude on the advance/retreat of glaciers and application to Himalayan glaciers is detailed in chapter 4. Application of the simple model to other basins is described in chapter 5 In chapter 6, preliminary work done on using the numerical ice-flow model to do future climate projections of glaciers is discussed.

Chapter 2

One-Dimensional glacier model

For simulating glaciers, numerical models of varying degrees of sophistication are possible (Kotlarski et al., 2010). Among them, Adhikari and Huybrechts (2009), used a simple model to simulate the variation of glacier AX010, and study scenarios for its future evolution. This simple model, based on a formulation due to Oerlemans (1988), seems to be quite effective in simulating the observed data over the past fifty years. We have developed a FORTRAN code based on the same formulation and that code has been used for all the simulations.

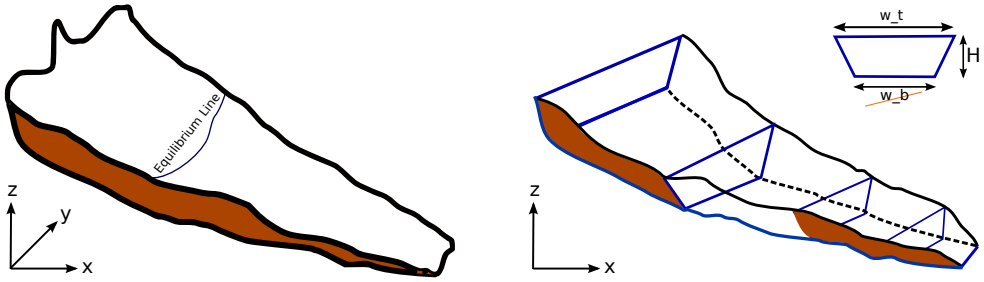

Figure 2.1: *Schematic of the geometry of a glacier (left panel) and the one-dimensional ice-flow model representation (right panel).*

.

Continuity equation for ice along the flow-line is

$$\frac{\partial}{\partial t}(\rho_{ice}A) + \frac{\partial}{\partial x}(\rho_{ice}UA) = \dot{B_{a\rho}} \tag{2.1}$$

where, A is the cross-sectional area, U is the ice-flow velocity, $\dot{B_{a\rho}}$ is the mass flow rate per unit-length and x is the co-ordinate along the centre-line.

If ice density does not vary with x, the above equation can be written as

$$\frac{\partial A}{\partial t} + \frac{\partial}{\partial x}(UA) = \dot{B}_a \tag{2.2}$$

where, $\dot{B}_a = \dot{B_{a\rho}}/\rho_{ice}$.

Assuming a trapezoidal cross-section , of base width w_b and top width $w_b + \lambda H$, where λ is the side-slope and H is the height, we get

$$A = \frac{1}{2}[w_b + (w_b + \lambda H)]H$$

Therefore

$$\begin{aligned} \frac{\partial A}{\partial t} &= \frac{\partial}{\partial t}([w_b + \lambda H/2]H) \\ &= w_b\frac{\partial H}{\partial t} + \frac{\partial}{\partial t}[\lambda H^2/2] \\ &= w_b\frac{\partial H}{\partial t} + \lambda H\frac{\partial H}{\partial t} \\ &= (w_b + \lambda H)\frac{\partial H}{\partial t} \end{aligned} \tag{2.3}$$

$$\tag{2.4}$$

Substituting the above expression in equation. 2.2, we get,

$$\begin{aligned} (w_b + \lambda H)\frac{\partial H}{\partial t} &= -\frac{\partial}{\partial x}(U[w_b + \lambda H/2]H) + \dot{B}_a \\ \implies \frac{\partial H}{\partial t} &= \dot{B}_l - \frac{1}{(w_b + \lambda H)}\frac{\partial}{\partial x}(U[w_b + \lambda H/2]H) \end{aligned} \tag{2.5}$$

where, $\dot{B}_l = \dot{B}_a/(w_b + \lambda H)$ with dimensions [L]/[T].

The velocity of ice U is split in to two components, the sliding velocity U_s and the deformation velocity U_d, which are modelled as follows

$$\begin{aligned} U &= U_s + U_d \\ &= \frac{f_s\tau^3}{H} + f_d\tau^3 H \end{aligned} \tag{2.6}$$

where τ is the shear stress and f_s, f_d are parameters to be derived from measurements and then tuned numerically.

τ is modelled as

$$\begin{aligned} \tau &= -(\rho_{ice}gH)\frac{\partial h}{\partial x} \\ &= -(\rho_{ice}gH)\frac{\partial}{\partial x}(h_b + H) \end{aligned} \tag{2.7}$$

where, g is the acceleration due to gravity, h is the elevation at the surface of the glacier and h_b is the elevation at the bottom/base of the glacier.

Substituting 2.6 and 2.7 in 2.5, we get

$$\begin{aligned}
\frac{\partial H}{\partial t} &= \dot{B}_l - \frac{1}{(w_b+\lambda H)}\frac{\partial}{\partial x}\left(\left(\frac{f_s\tau^3}{H} + f_d\tau^3 H\right)[w_b+\lambda H/2]H\right) \\
&= \dot{B}_l - \frac{1}{(w_b+\lambda H)}\frac{\partial}{\partial x}\left((f_s+f_dH)[w_b+\lambda H/2](\tau^3)\right) \\
&= \dot{B}_l + \frac{1}{(w_b+\lambda H)}\frac{\partial}{\partial x}\left((f_s+f_dH)[w_b+\lambda H/2]\left[\rho_{ice}gH\frac{\partial}{\partial x}(h_b+H)\right]^3\right) \\
&= \dot{B}_l + \frac{1}{(w_b+\lambda H)}\frac{\partial}{\partial x}\left((\rho_{ice}gH)^3(f_s+f_dH)[w_b+\lambda H/2]\left[\frac{\partial}{\partial x}(h_b+H)\right]^3\right) \quad (2.8)
\end{aligned}$$

This is a non-linear equation involving third power of the spatial derivative of H. To make the numerical solution well posed, it is recast as a diffusion equation, by freezing part of the second term on the RHS, smoothing it and retaining derivatives up to the second order.

$$\begin{aligned}
\frac{\partial H}{\partial t} &= \dot{B}_l + \frac{1}{(w_b+\lambda H)}\frac{\partial}{\partial x}\left((\rho_{ice}gH)^3(f_s+f_dH)[w_b+\lambda H/2]\left[\frac{\partial}{\partial x}(h_b+H)\right]^2\left[\frac{\partial}{\partial x}(h_b+H)\right]\right) \\
&= \dot{B}_l + \frac{1}{(w_b+\lambda H)}\frac{\partial}{\partial x}\left(D\left[\frac{\partial}{\partial x}(h_b+H)\right]\right)
\end{aligned} \quad (2.9)$$

where

$$D = (\rho_{ice}gH)^3(f_s+f_dH)[w_b+\lambda H/2]\left[\frac{\partial}{\partial x}(h_b+H)\right]^2 \quad (2.10)$$

The mass balance, which is a function of x and t is modelled as follows

$$B_l(x,t) = \alpha(h(x) - h_{EL}) + B_{l-hist}(t) \quad (2.11)$$

where h_{EL} is the equilibrium line altitude, α is estimated from historical data and $B_{l-hist}(t)$ has to be specified either from observations or using some proxy data.

The historical variation of mass balance is taken to be a linear function of either the temperature anomaly ΔT or precipitation anomaly ΔP.

$$B_{l-hist}(t) = C_1\Delta T(t) + C_2$$

or

$$B_{l-hist}(t) = C_3\Delta P(t) + C_4$$

The original form, equation 2.5 with U specified, is an advection equation and is a hyperbolic PDE. With the inclusion of the model for U and grouping of the terms as in equation 2.9, it becomes a diffusion equation (parabolic). The second form appears to be more well posed and is adopted for numerical solution.

The code for numerical solution of the model equations is given in Appendix A. It is written in FORTRAN 90 and takes around 0.025 seconds per year of integration on a typical workstation.

2.0.1 Input data required

The inputs needed by the 1-D model are listed in table 2.1.

width of base of glacier	$w_b(x)$
Side-slope	$\lambda(x)$
elevation of glacier bed	$h_b(x)$
mass balance	$B_{l-hist}(t)$
coefficient (B versus h)	α
coefficients (B versus T)	C_1, C_2
equilibrium line altitude	h_{EL}

Table 2.1: *Inputs required by the numerical model*

These fields are not directly measured and can be obtained in the following manner.

- *Topographic map/ Digital elevation map*:
  Using this the width of glacier surface (w_t) and elevation of glacier surface (h) can be calculated.

- *Equilibrium line altitude* (h_{EL}).

- *Ice thickness (H)* at a few locations on the glacier (from GPR):
  Using this the elevation of glacier base can be calculated ($h_b = h - H$)

- *Mass balance* at a few locations (different heights) on the glacier:
  Using this the constant α can be estimated.

- *Historical variation of temperature/precipitation* at a station close to the glacier and *net mass balance* for a few years:
  Using this the constants C_1 or C_3 can be estimated. C_2 and C_4 are tuned to match observed lengths.

Parameter	Units	Typical value
f_s	$Pa^{-3}yr^{-1}$	1.8×10^{-12}
f_d	$Pa^{-3}yr^{-1}$	6.0×10^{-17}
α	yr^{-1}	0.01
$\lambda(x)$	–	1

Table 2.2: *Values of parameters and constants used in AH2009*

2.1 Validation

The same case AX010 was simulated using The values of the parameters and other inputs are listed in Appendix B. The mass balance was specified as a function of time in a manner identical to AH2009 (Data present in appendices of Adhikari 2007). The model integration was started from the year 1200, with zero ice thickness and spun up till 1600 with a constant mass balance. It was then forced with mass balance variation as described in AH2009 (figure 5b).

Glacier heights as a function of x at various times from 1600 to 2005 are plotted in figure 2.2. The advance from 1600 and reaching of a peak around 1850 and subsequent retreat can be seen clearly.

The typical values of f_s, f_d are listed in table 2.0.1. In addition, AH2009 mention that these were multiplied by a factor $(1/\gamma)$ to match the results with observations. The values of γ used by them range from 2.5 to 30. We find that a factor of 3.25 gives the best match.

The variation of the glacier length with time is shown in figure 2.3. Figure 5 of AH2009 is also shown for comparison. One can see that the match is quite good.

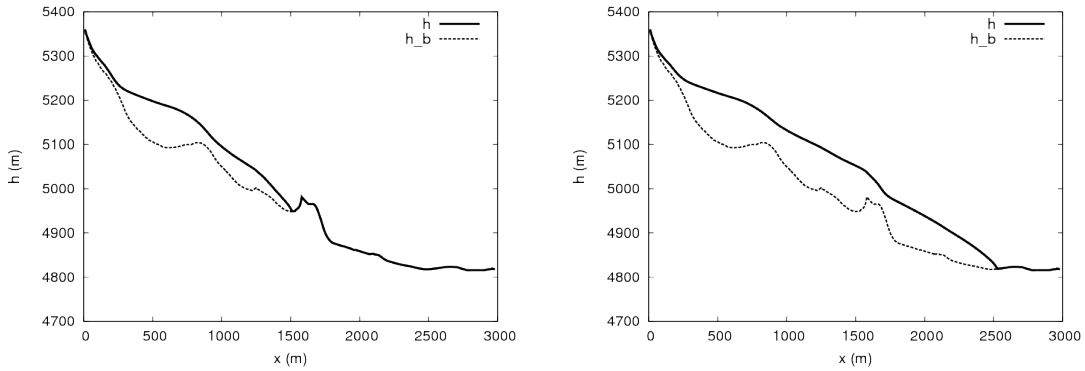

(a) 1600 (b) 1850

(c) 1950 (d) 2005

Figure 2.2: *Simulated variation of glacier heights with time.*

.

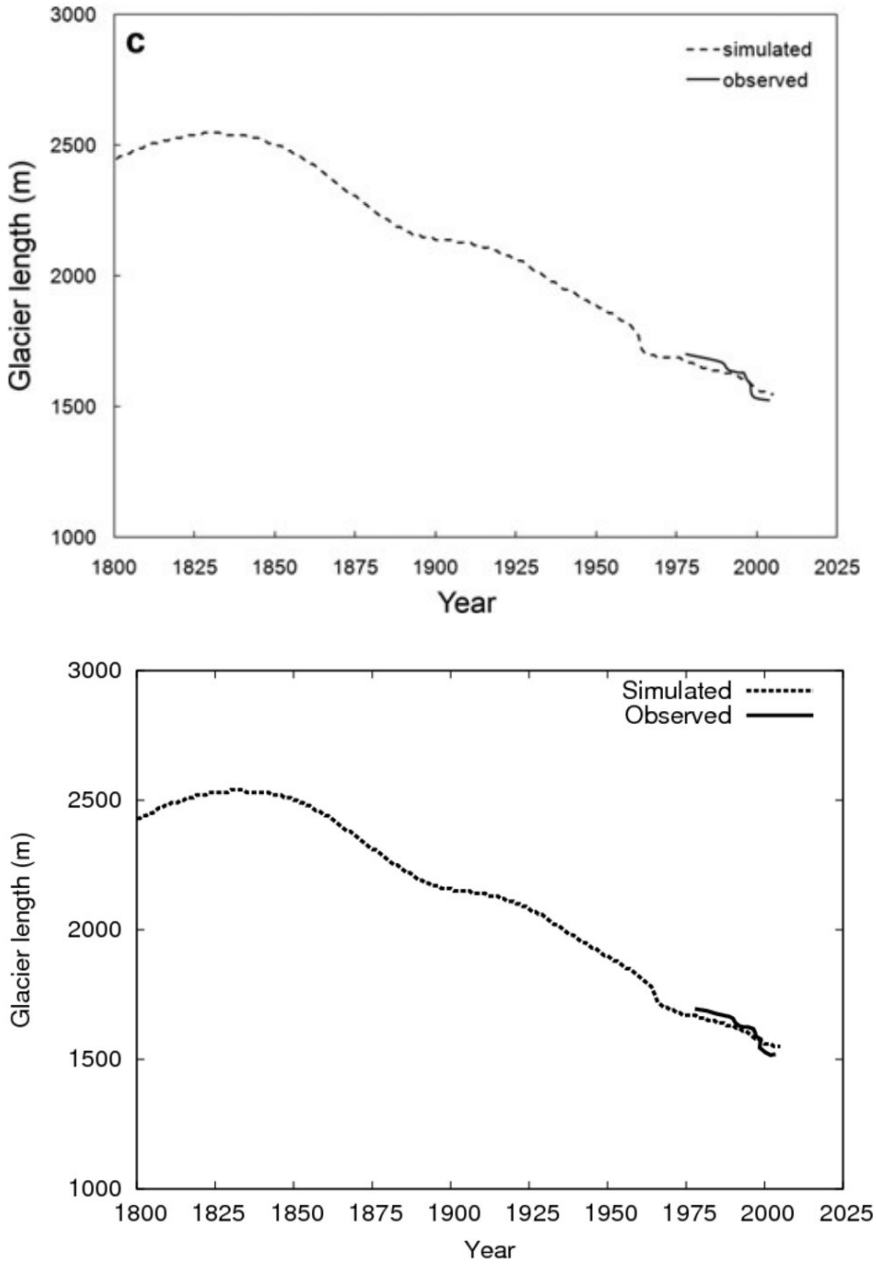

Figure 2.3: *Simulated variation of glacier length with time. top panel: Figure 5 of A-H-2009, bottom panel: present computation*

.

Chapter 3

Model problem

For an understanding of the basic dynamics, we consider a constant width glacier, with constant bed-slope and zero mass balance.

The simulation was started with a block of ice of length L_0 and uniform thickness H_0 and with the mass balance term set to zero. Schematic view of the process is shown in figure 3.1. L_0 was varied from 2 to 6 km. and H_0 varied from 50 to 250 metres. The model was integrated for upto 2000 years to understand the qualitative behavior.

The variation of the ice-thickness H as a function of x at different times can be seen in Figure 3.2. One can see that the initial top-hat profile spreads out with time and becomes smoother due to the diffusive processes. At later times, the shape becomes self-similar. An interesting aspect is that the left end seems to be pinned to a point close to the initial location of the block, even though the boundary condition is imposed at $x = 0$. This is because of a balance between the gravity which tends to move the ice towards the right and the gradient of the ice-surface which induces a negative velocity.

Variation of the block length and maximum thickness with time is shown in Figure 3.3 for different slopes. The block length, increases rapidly at $t = 0$ and then nearly linearly. For higher slopes, the increase is more. The maximum thickness decreases with time, since total ice-mass has to be conserved.

Since we are interested in the movement, the ice-front velocity is plotted as a function of time in figure 3.4. The velocity multiplied with $\sqrt{t}$ is almost constant for large times (figure 3.5) indicating that $L(t) \sim \sqrt{t}$.

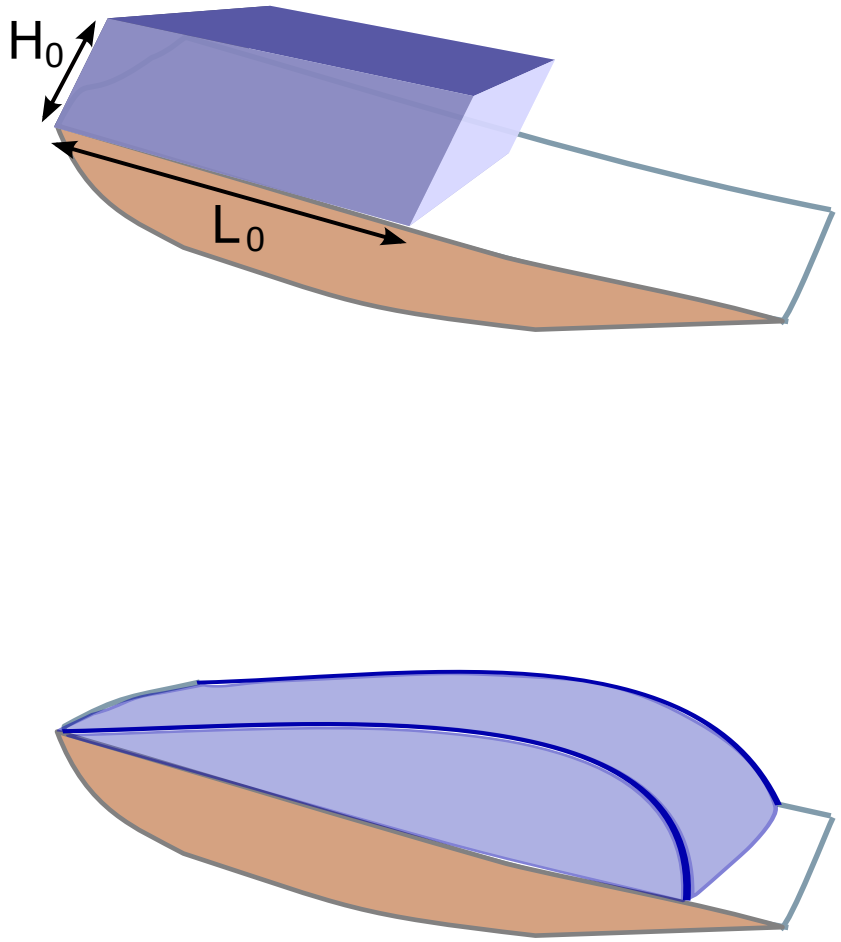

Figure 3.1: *Schematic view of the movement of a block of ice on an incline, with no snowfall or melting. Top panel: Initial configuration with length L_0 and thickness H_0. Bottom panel: The block at a later time t. The block continues to flow, becoming longer and thinner.*

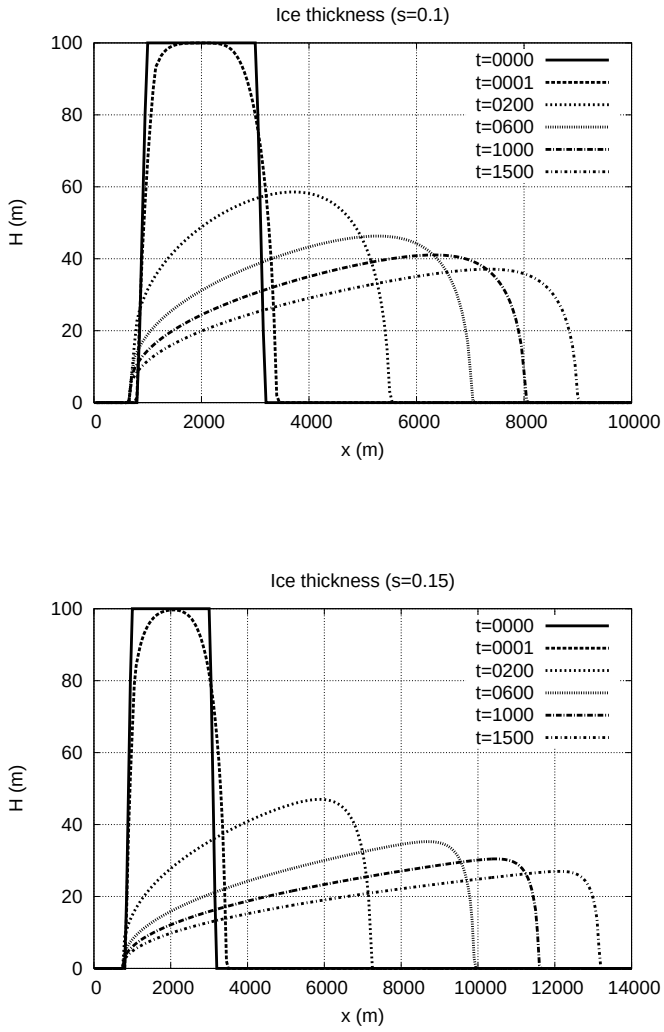

Figure 3.2: *Variation of the ice thickness with length at different times for slopes of 0.10 and 0.15*

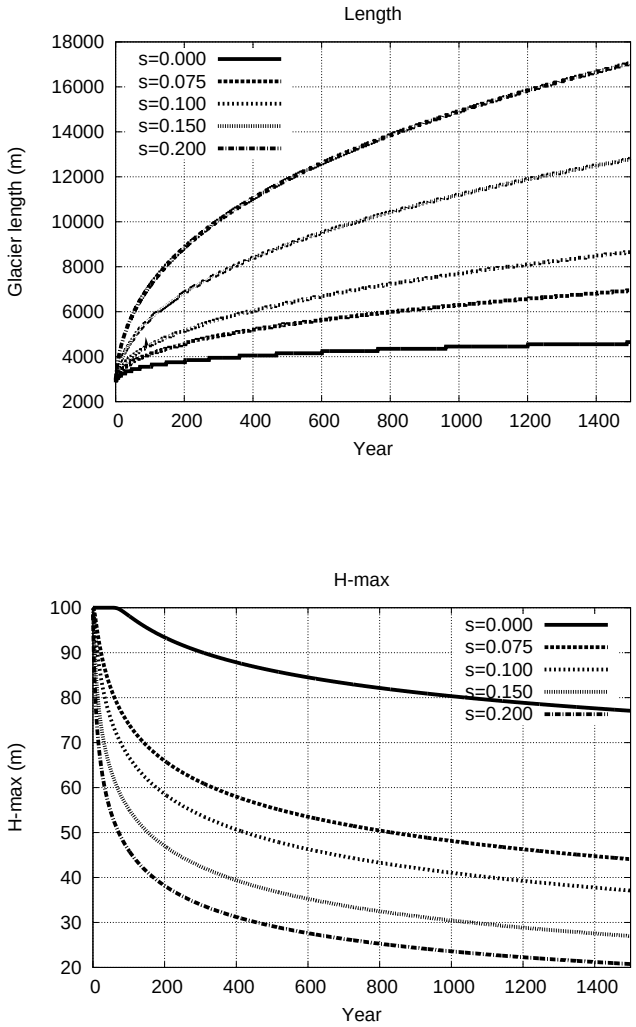

Figure 3.3: *Variation of the block length and maximum thickness with time for different slopes*

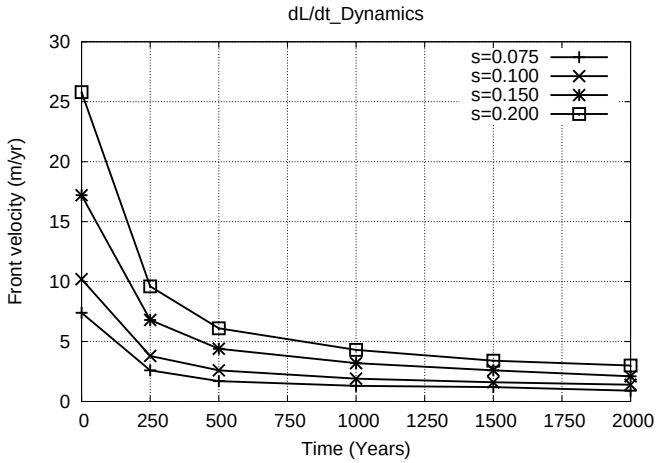

Figure 3.4: *Variation of ice-front velocity with time for different slopes*

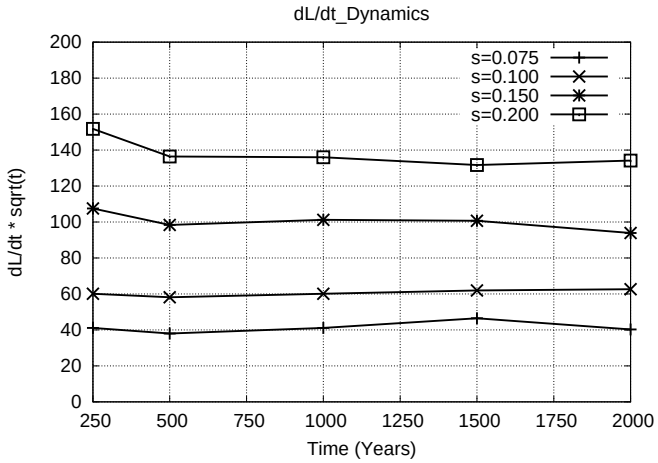

Figure 3.5: *Variation of scaled ice-front velocity with time for different slopes*

3.1 Analytical solutions

The velocity of ice U is modelled as follows

$$U = \frac{f_1 \tau^n}{H} \tag{3.1}$$

where τ is the shear stress and f_1 a parameter (assumption: velocity due to sliding dominates), and $n = 1, 3$

τ is modelled as

$$\tau = -(\rho_{ice} g H) \frac{\partial}{\partial x}(h_b + H) \tag{3.2}$$

where, g is the acceleration due to gravity, h is the elevation at the surface of the glacier and h_b is the elevation at the bottom/base of the glacier.

$$\begin{aligned} & \frac{\partial H}{\partial t} + \frac{\partial}{\partial x}\left[\left(-(\rho_{ice} g) f_1 \frac{\partial}{\partial x}(-s + H)\right)^n\right] = 0 \\ \implies \quad & \frac{\partial H}{\partial t} + n f_1 (-\rho_{ice} g)^n H^{n-1} \left[-s + \frac{\partial H}{\partial x}\right]^{n-1} \left[-s \frac{\partial H}{\partial x} + \frac{\partial}{\partial x}\left(H \frac{\partial H}{\partial x}\right)\right] = 0 \end{aligned} \tag{3.3}$$

3.2 Case: $n = 1$

$$\begin{aligned} & \frac{\partial H}{\partial t} - \rho_{ice} g f_1 \left[-s \frac{\partial H}{\partial x} + \frac{\partial}{\partial x}\left(H \frac{\partial H}{\partial x}\right)\right] = 0 \\ \implies \quad & \frac{\partial H}{\partial t} + \rho_{ice} g f_1 s \frac{\partial H}{\partial x} = \rho_{ice} g f_1 \frac{\partial}{\partial x}\left(H \frac{\partial H}{\partial x}\right) \end{aligned} \tag{3.4}$$

3.2.1 Quadratic form solution

$$H(x,t) = C_3 \left|t + C_1\right|^{-1/3} - \frac{(x - \rho g f_1 s t + C_2)^2}{6 \rho g f_1 (t + C_1)} \tag{3.5}$$

For a quadratic hump with initial length L_0 and height H_0,

$$H(x,t) = \frac{H_0}{(1 + t*)^{1/3}} \left[1 - \frac{(x * -1 - (s/S_0) t*)^2}{(1 + t*)^{2/3}}\right] \tag{3.6}$$

where $t* = t/t_1$ $t_1 = (L_0^2)/(24H_0\rho g f_1)$,
$x* = x/(L_0/2)$, $S_0 = 12H_0/L_0$

Maximum height scales as follows

$$H_{max}(t) = \frac{H_0}{(1+t*)^{1/3}} \tag{3.7}$$

Length scales as follows

$$L(t) = L_0\,(1+t*)^{1/3} \tag{3.8}$$

Area is conserved.

3.2.2 Approximation 1

If the variation of H is small over a major portion of the initial (and later) profiles,

$$\frac{\partial H}{\partial t} + \rho_{ice} g f_1 s \frac{\partial H}{\partial x} = \rho_{ice} g f_1 \frac{\partial}{\partial x}\left((\bar{H} + \epsilon() + .)\frac{\partial H}{\partial x}\right) \tag{3.9}$$

To first order,

$$\frac{\partial H}{\partial t} + \rho_{ice} g f_1 s \frac{\partial H}{\partial x} = \rho_{ice} g f_1 \bar{H} \frac{\partial^2 H}{\partial x^2} \tag{3.10}$$

This is a linear convection-diffusion equation of the form,

$$\frac{\partial H}{\partial t} + c\frac{\partial H}{\partial x} = d\frac{\partial^2 H}{\partial x^2} \tag{3.11}$$

where $c = \rho_{ice} g f_1 s$ and $d = \rho_{ice} g f_1 \bar{H}$.

If $H(x,0) = H_0$, $0 \le x \le L_0$ and 0 elsewhere, the exact solution is

$$H(x,t) = \frac{H_0}{2}\left[erf\left(\frac{x-ct}{\sqrt{4dt}}\right) - erf\left(\frac{x-L_0-ct}{\sqrt{4dt}}\right)\right] \tag{3.12}$$

Maximum height (at $x = L_0/2 + ct$) scales as follows

$$\begin{aligned} H_{max}(t) &= H_0 erf\left(\frac{L_0}{4\sqrt{dt}}\right) \\ &\sim \frac{H_0 L_0}{4\sqrt{dt}} \qquad \text{for large t} \end{aligned} \tag{3.13}$$

The length (where the function reaches 1% of its maximum value) is

$$L_{99} = L_0 + ct + 4\sqrt{dt}$$

Since $c < d$ initial behaviour is like $\sqrt{t}$ and later like t

3.3 Case: $n = 3$

$$\frac{\partial H}{\partial t} - 3f_3(\rho_{ice}g)^3 H^2 \left[-s + \frac{\partial H}{\partial x}\right]^2 \left[-s\frac{\partial H}{\partial x} + \frac{\partial}{\partial x}\left(H\frac{\partial H}{\partial x}\right)\right] = 0 \tag{3.14}$$

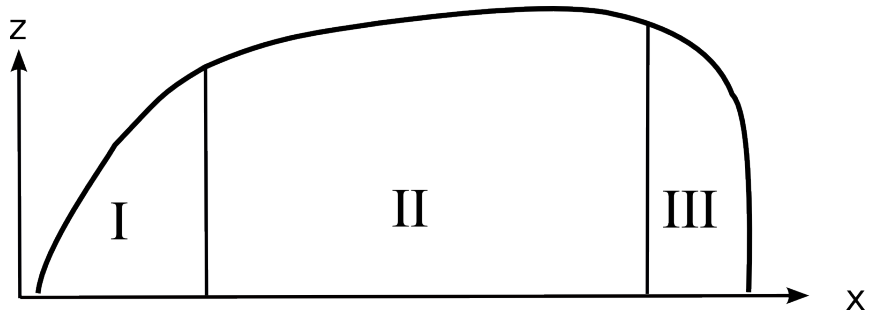

Region II

$$\frac{\partial H}{\partial x} << s; H \sim \bar{H}$$

$$\frac{\partial H}{\partial t} + c_g\frac{\partial H}{\partial x} = d_g\frac{\partial^2 H}{\partial x^2} \tag{3.15}$$

where $c_g = 3(\rho_{ice}g)^3 f_3 s^3 \bar{H}^2$ and $d_g = 3(\rho_{ice}g)^3 f_3 s^2 \bar{H}^3$.

Region I

$$\frac{\partial H}{\partial x} \sim 1; \qquad ; s\frac{\partial H}{\partial x} \sim \left(\frac{\partial H}{\partial x}\right)^2$$

$$\frac{\partial H}{\partial t} = K_1 H^3 \frac{\partial^2 H}{\partial x^2} \tag{3.16}$$

where $K_1 = 3(\rho_{ice}g)^3 f_3(1-s)^2$.

Similarity solution

$$H(x,t) = \left[\frac{3(x-A)^2}{2K_1(t+B)}\right]^{1/3} \tag{3.17}$$

With the conditions $H(0,t) = 0$ and $H(L_0/2, 0) = H_0$

$$H(x,t) = \left[\frac{x^2}{2(\rho g)^3(1-s)^2(t+3L_0^2/4H_0^3)}\right]^{1/3} \tag{3.18}$$

Region III

$$\frac{\partial H}{\partial x} \sim -1; \qquad ; s\frac{\partial H}{\partial x} \sim \left(\frac{\partial H}{\partial x}\right)^2$$

$$\frac{\partial H}{\partial t} = K_2 H^3 \frac{\partial^2 H}{\partial x^2} \tag{3.19}$$

where $K_2 = 3(\rho_{ice}g)^3 f_3(1+s)^2$.

Similarity solution

$$H(x,t) = \left[\frac{3(x-A)^2}{2K_2(t+B)}\right]^{1/3} \tag{3.20}$$

With the conditions $H(L,t) = 0$ and $H(L_0/2, 0) = H_0$

$$H(x,t) = \left[\frac{(x-L)^2}{2(\rho g)^3(1+s)^2(t+3L_0^2/4H_0^3)}\right]^{1/3} \tag{3.21}$$

$$L = L_0 + c_g t + 4\sqrt{d_g t}$$

3.3.1 Approximation 2

Very close to origin (part of region I)

$$s << \frac{\partial H}{\partial x} \Longrightarrow \frac{\partial H}{\partial t} \sim 0$$

Therefore

$$\begin{aligned} & \frac{\partial}{\partial x}\left(H\frac{\partial H}{\partial x}\right) = 0 \\ \implies \quad & \frac{\partial H^2/2}{\partial x} = 0 \end{aligned} \tag{3.22}$$

Solution (with b.c $H(0,t) = 0$)

$$H(x,t) = \sqrt{C_1 x} \tag{3.23}$$

Chapter 4

Movement of glaciers: Relative effect of slope and equilibrium line altitude on the retreat of Himalayan glaciers

Numerous investigations have been carried out to understand changes in glaciers in the Himalayas (Kulkarni et al., 2011; Bolch et al., 2010; Yong et al., 2010). These investigations show that a majority of glaciers in the Himalaya are retreating. However recent investigations in Karakoram mountain range indicate that some glaciers are advancing (Scherler et al., 2011). In addition, rate of retreat is different for individual glaciers depending upon numerous geomorphological parameters like area-altitude distribution, length, size, slope, debris cover etc. (Deota et al., 2011; Kulkarni et al., 2005). Field observations carried out in a large glacier like Siachen have shown that the glacier is almost stationary or has shown little retreat since 1995. This has lead to the erroneous conclusion that glaciers in the North-West Himalayas are not affected by global warming (Ganjoo and Kaul, 2009).

In our opinion, the different rates of retreat/advance of glaciers within a region, over which the climatic conditions do not change significantly, is due to the important role played by the dynamics of ice movement, which in turn is controlled by the mean slope and length of the glacier. In this chapter, we provide an explanation for this apparent contradiction of advancing glaciers in a global warming scenario, by using a simple model to understand relative importance of slope, length, and Equilibrium Line Altitude (ELA). ELA is considered as a good indicator of glacier mass balance (Benn and Lehmkul, 2000). The model shows that rate of retreat of glaciers can be different even if environmental changes are similar in a given region. This is done without explicitly using the concepts of inertia and response time of a glacier.

In what follows, mean slope s is defined as follows

$$s = \frac{h_{max} - h_{min}}{L}$$

where h_{max} is the altitude at the top of the glacier, h_{min} is the altitude at the snout and L is the length of the glacier. Schematic view is shown in figure 4.1.

4.1 Motivation and Hypothesis

The role of the mean-slope in determining equilibrium lengths of glaciers is well known. Using simple arguments, one can derive an expression for the equilibrium length, in terms of the slope, equilibrium line altitude and mean thickness (Oerlemans, 2008). Change in any of these parameters would result in advance/retreat. Empirical evidence of the role of slope is also available. In figure 4.2, we show the variation of retreat rates of glaciers in the Parbati and Baspa basins with mean slope. The retreat rates were derived over a 11 year time period from satellite images. One can see that there is a trend of decreasing retreat rate with increasing slope. This set had only retreating glaciers and can be assumed to have nearly the same change in environmental condition (like change in ELA). In addition, it can be seen that the variability decreases with increasing slope, suggesting that the slope has a major role to play.

Using the more extensive satellite data of Scherler etal, 2011, the distribution of retreat rates for low slopes ($s < 0.15$)) and high slopes ($s > 0.25$) are plotted in figure 4.3. A limitation of this dataset is that it is available for eight years, in which inter-annual and short-term variation would also be seen. For low slopes, the maxima is at -10 m/yr while for large slopes the maxima is a 0 m/yr with more advancing glaciers. This suggests that slope in addition to the climate sensitivity term $1/s$, there is another part proportional to s contributing to the advance.

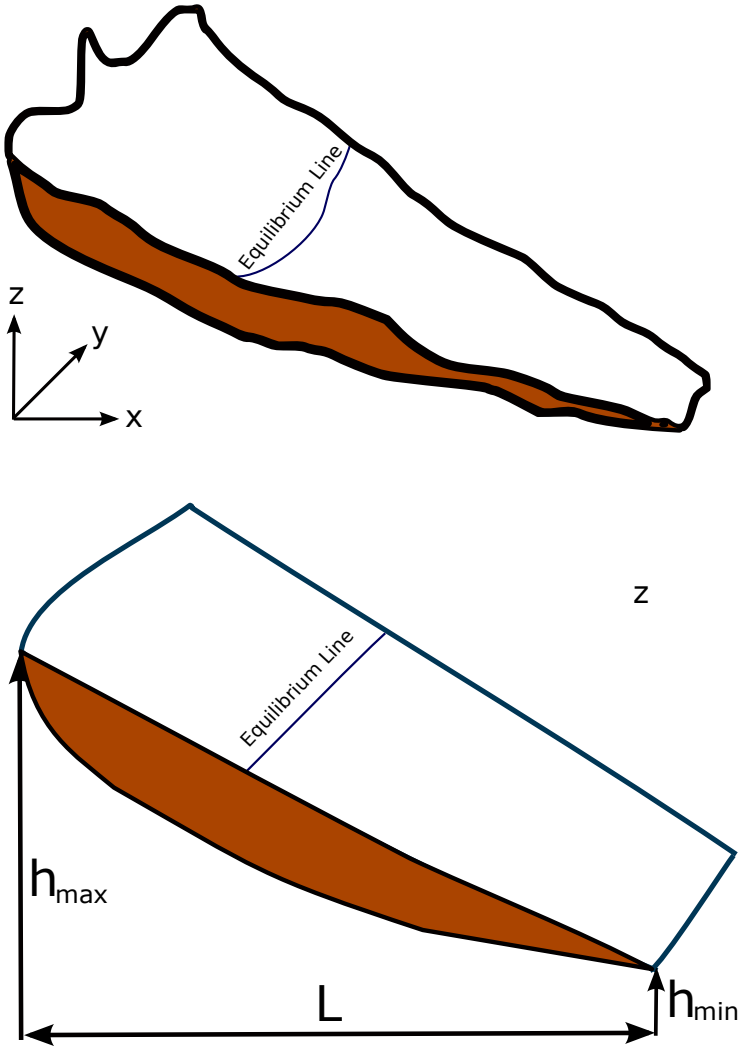

Figure 4.1: *Schematic view of a glacier and an idealized version (incline with same mean slope)*

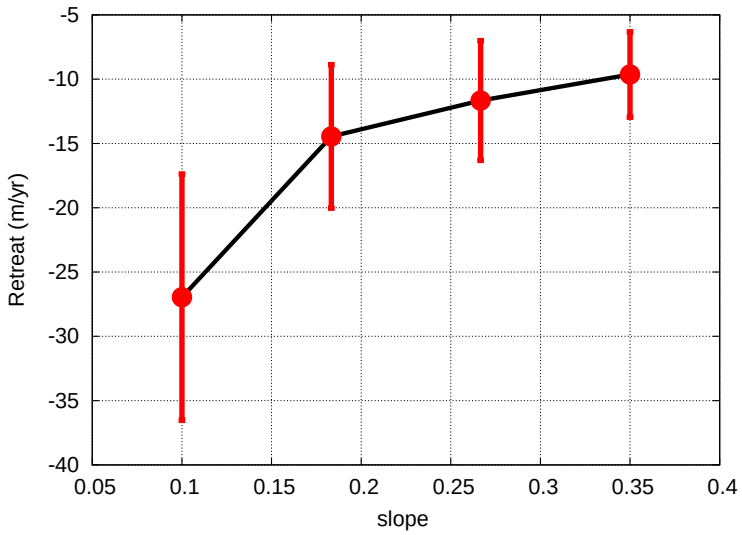

Figure 4.2: *Observed variation of retreat rates with slope, for glaciers in the Parbati and Baspa basins. The solid circle represents the mean value and bars, the standard deviation. The set consists of 57 glaciers.*

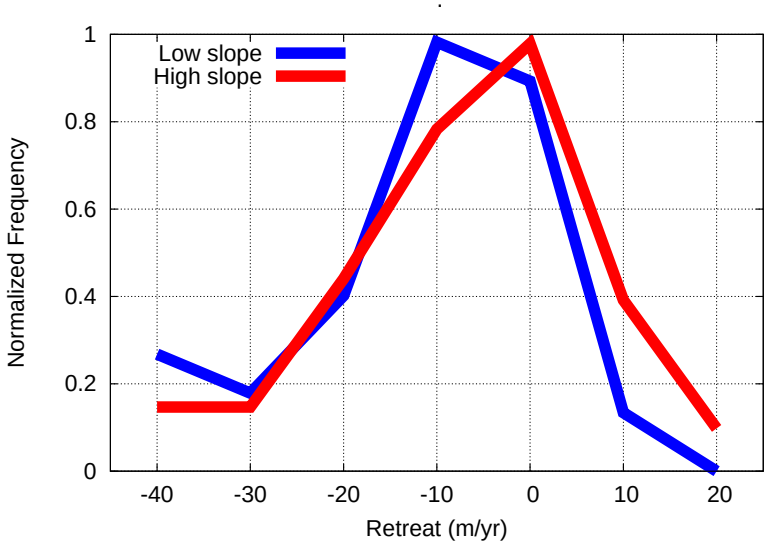

Figure 4.3: *Distribution of retreat rates for low slope (< 0.15) and high slope (> 0.25) glaciers in the Himalayas. Data is taken from Scherler etal 2011. The sets consist of 64 and 61 glaciers respectively.*

The slope, in addition to determining the sensitivity to changes in ELA can also influence the advance due to dynamics. A commonly used equation for glacier simulations (Oerlemans, 1988; Adhikari and Huybrechts, 2009) is of the following form.

$$\frac{\partial H}{\partial t} = \underbrace{\dot{B}_l} \underline{-\frac{\partial}{\partial x}(UH)} \tag{4.1}$$

where, $H(x)$ represents the thickness at a point x along the flow-line, $U(x)$ the mean velocity of ice along the flow-line and $\dot{B}_l$ is the mass balance with dimensions [L]/[T].

The mass balance term (with underbraces) is a function of the altitude and climate forcing and is prescribed as a function of x and t. The other term (underlined) depends on the velocity U which is a function of the shear-stress, which depends mainly on the bottom and surface slopes and parameters which represent basal slip and sliding. The first term represents the thermodynamics (snowfall, melting) and the second the dynamics (gravity, slope effects). The net movement (advance/retreat) of the glacier front is due to the integrated effect of both the processes. Given that gravity is always present, one can consider the following scenarios

1. The mass balance term is significant and unchanging: The system would evolve to a steady state, wherein the accumulation, ablation and flow are in balance. This is the usual equilibrium scenario.

2. The mass balance term is negligible (this is a hypothetical situation): In this case, the ice would flow down the slope due to gravity. This can also be thought of as the limiting case where the thermodynamic processes are unimportant and only ice dynamics, controlled by the slope is the relevant process.

In the first case changes to the glacier length are possible only if the external conditions (mass balance) change with time. In the second case, the glacier would continue to advance, with the thickness reducing (since volume is conserved). Our hypothesis is that the advance/retreat of a glacier can be understood in terms of theses two tendencies and that they can be added linearly.

The following assumptions are made

1. While local conditions could vary, the large-scale environmental forcing (global temperature change, overall snowfall change) on all the glaciers, in the region considered, is similar.
2. Retreat/advance is a balance between two opposing tendencies
   (a) advance due to gravity (dL/dt_{dynamics}), which includes both ice-deformation and sliding (controlled primarily by length and mean slope) and
   (b) retreat due to increased elevation of the equilibrium line ($dL/dt_{\text{thermodynamics}}$) (which depends on changes in snowfall/melting)

It is proposed that the overall retreat is then

$$\begin{aligned} \left.\frac{dL}{dt}\right|_{glacier} &= \left.\frac{dL}{dt}\right|_{dynamics} + \left.\frac{dL}{dt}\right|_{thermodynamics} \\ &= \alpha F_1(L,H,s) + \frac{dL}{dh_e}\frac{dh_e}{dt} \end{aligned} \tag{4.2}$$

The first term is the tendency of the glacier front to advance due to gravity, which includes both ice-deformation and sliding. This is the new idea proposed in this work. The second term, is equivalent to the climate sensitivity of glacier length to ambient air temperature (dL/dT) as derived by Oerlemans (2008), multiplied by the rate of change of temperature with time. The effect of the two processes is assumed to be linear and the net advance/retreat is the sum of the two.

F_1 is a function of L, H and s and is obtained from ice-flow simulations. dL/dh_e is estimated from equilibrium simulations. dh_e/dt is related to the environmental change and is expected to be related to the rate of increase of mean global temperature.

Given the lengths, slopes and retreat rates for a set of real glaciers, one can then find a least-squares, best-fit estimate of α and dh_e/dt. These values can then be used to predict the retreat/advance for other glaciers. One can also use it to understand the contribution of different terms to the advance/retreat.

This way of splitting the change in glacier length is different from the manner it is done in simple models, Cuffey and Patterson (2010), for the accumulation zone, ablation zone or at the glacier terminus. In those models, the mass balance component and ice-flow term are both present, leading to a linear system, which responds to an abrupt change in environmental changes. In our model, the thermodynamics and dynamics processes are split. To the best of our knowledge this particular way of decomposing the change in the length of the glacier has not been done before.

For the numerical simulations, we have used the FORTRAN code, we developed, based on the formulation of Adhikari and Huybrechts (2009) (details in chapter 2 and appendix A). While Adhikari and Huybrechts (2009) have used their numerical model to simulate the historical variation of particular glaciers and project the future scenarios, we have used the model in a different way. We use it primarily to simulate idealized glacier flow at two extreme conditions: a) with zero mass balance and b) equilibrium conditions.

4.2 Impact of slope

For medium to large glaciers (length > 1.5 km), the mean-slope and length are expected to play a major role, therefore we ignore variations of the bed topography and perform idealized simulations with the base varying linearly and consider different slopes.

The first set of ice-flow simulations were performed with zero mass balance. This was done to simulate the gravity effects on a mass of ice and quantify the part of motion of glaciers which is due to just flow down the incline, in the absence of snowfall/melting. Such a flow does not occur in nature, since some mass balance is always present. However, these simulations provide an indication of the tendency of a mass of ice to flow and we use the initial trend (after one year) to estimate F_1 as a function of L, H and s.

In the second set, mass balance varying as a linear function of altitude was imposed and simulations performed varying the equilibrium line altitude, keeping the origin of the glacier constant. An assumption here is that for glaciers considered, it is only difference $h_{max} - h_{ELA}$ which matters.

4.2.1 Ice-flow simulations

Results of ice-flow simulations, with no snowfall or melting, which were performed to estimate F_1 as a function of L, H and s, are presented in this section. The simulation was started with a block of ice of length L_0 and uniform thickness H_0 and with the mass balance term set to zero. L_0 was varied from 2 to 6 km. and H_0 varied from 50 to 250 metres. The qualitative long-term behavior has already been described in chapter 3. For the current, study, the velocity at initial stages, i.e. after one year was used.

It should be noted that the functional form of F_1, i.e the dependence on L, H and s is not affected by the time at which the front velocity is chosen. Only the constant of multiplication changes.

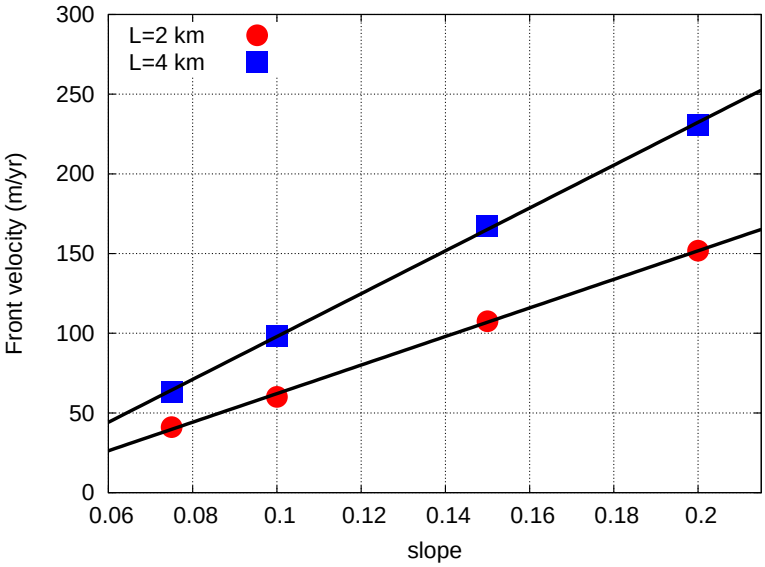

Figure 4.4: *Variation of velocity of the front as a function of slope for two different values of* L_0.

Initially, the thickness has a top-hat profile and soon, the diffusive processes make the distribution smooth, with a maxima towards the lower end. The gravitational force causes the ice mass to stretch and flow down the incline. Initially, the length increases sharply with time and later there is nearly linear growth. The rate of change increases with the slope. The maximum thickness decreases with time and falls more rapidly with increasing slope. The effect of the mean slope on the dynamics is to increase the average ice-velocity. The velocity of the front increases with slope and decreases gradually with time.

For application to real glaciers, the value of dL/dt after one year, given the length and thickness at the end of the previous year is used. On varying L_0, the velocity was found to increase linearly. The dependence on H_0 was found to follow a three-fourths power law. The variation with s was found to be linear. The following expression was found to be a good fit for the simulated values of dL/dt.

$$F_1(L, H, s) = sL(H)^{3/4} \tag{4.3}$$

where L is in kilometres, H is in metres and dL/dt in metres/year.

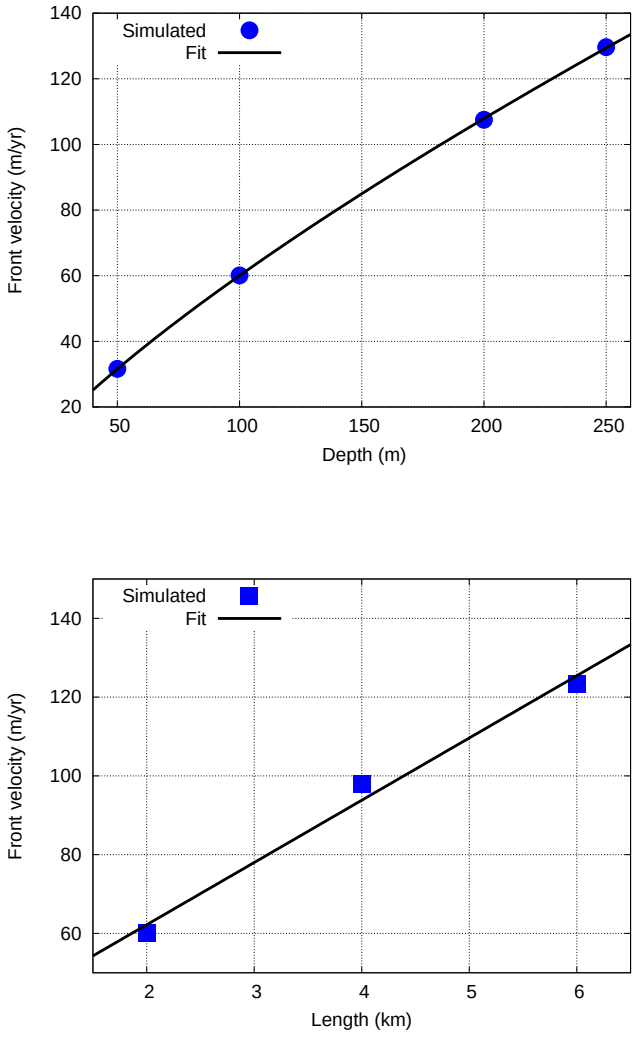

Figure 4.5: *Top panel: Variation of velocity of the front as a function of thickness H_0 with slope and L_0 kept constant. Bottom panel: Variation of velocity of the front as a function of thickness L_0 with slope and H_0 kept constant.*

4.2.2 Equilibrium mass balance simulations

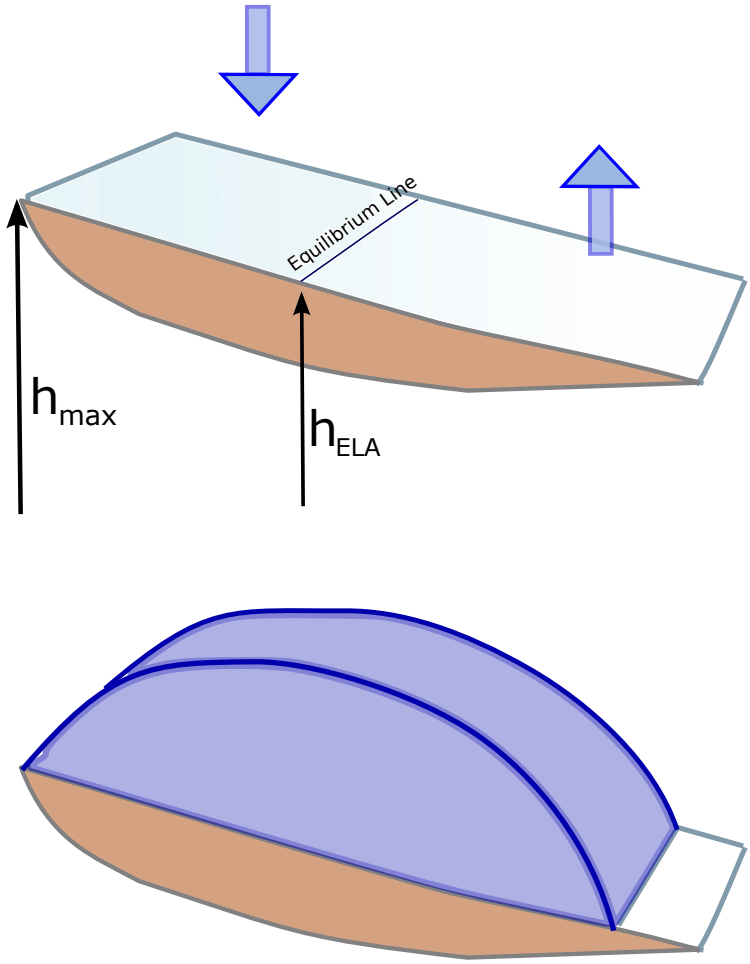

Figure 4.6: *Schematic view of the equilibrium shape of a glacier on an incline with snowfall and melting. The mass-balance distribution is linear with altitude. Left panel: Initial configuration with no ice. Right panel: Equilibrium shape of the glacier.*

Results of simulations with mass balance are presented in this section. Objective was to estimate dL/dh_e and average thickness H as functions of L and s. The simulations were started with zero ice and integrated with a specified gradient balance β. Once the steady state was reached, the equilibrium length and thickness were determined. Schematic view of the process is shown in figure 4.6.

Observed equilibrium line altitudes, lengths and mean slopes for a few Himalayan glaciers are listed in table 4.1. Therefore simulations were performed for slopes varying

from 0.075 to 0.2 and $h_{max} - h_{ELA}$ from 0 to 1600. The value of β used by Adhikari and Huybrechts is 0.01. For Chhota Shigri, the value was estimated to be 0.009. Since these values are quite close, the simulations were performed with $\beta = 0.009$.

For convenience, we define

$$h_e = h_{max} - h_{ELA}$$

Glacier	s	h_e (m)	L (km)	Retreat (m/yr)	Source
AX010	0.180	150	1.5	-6.50	Adhikari etal 2009
Hamtah	0.102	300	7.0	-16.00	Siddiqui etal 2005
Ch-Shigri[1]	0.140	470	9.0	-7.17	Swaroop etal 1999
Satopanth	0.150	1200	14.0	-8.30	Nainwal etal 2008
B-K[2]	0.120	1330	17.0	-7.30	Nainwal etal 2008

Table 4.1: *Observed values of slope, $h_e = h_{max} - h_{ELA}$ and length for a few Himalayan glaciers.* [1]*: Ch-Shigri == Chhota Shigri and* [2]*: B-K == Bhagirath-Kharak.*

With linear variation of mass balance with altitude (gradient $\beta = 0.009$) and zero net mass balance, equilibrium shapes on varying base slope and h_e are as follows.

The equilibrium values of length increase with h_e (figure 4.7). Also, one can see that for the same value of h_e, the length decreases with increasing slope.

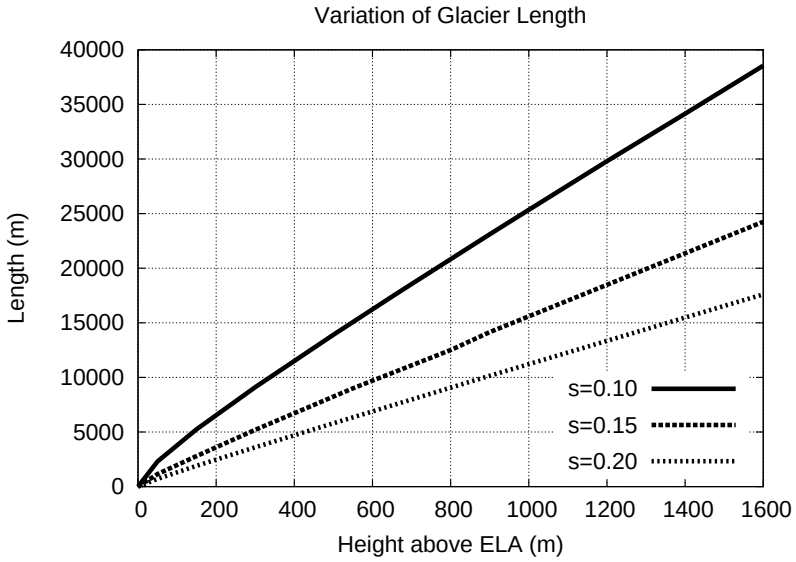

Figure 4.7: *Variation of equilibrium length as function of h_e and s.*

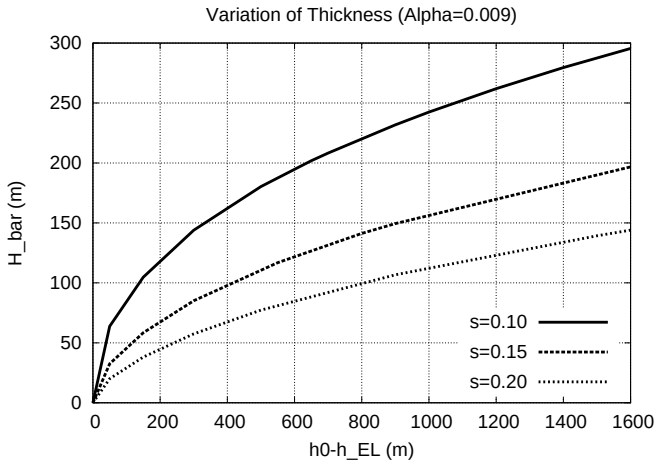

Figure 4.8: *Variation of thickness as function of h_e and s.*

Oerlemans (2008) derived the following estimate for equilibrium length.

$$L = \frac{2}{s}\left(h_{max} - h_{EL} + H_m\right) = \frac{2}{s}\left(h_e + H_m\right) \tag{4.4}$$

where H_m is the average thickness. For large L the term $2H_m/s$ is small and the slope is approximately $2/s$. On comparing the two expressions and the values from the graph, for $L > 1$ km, the following expression serves as a good approximation

$$\frac{dL}{dh_e} = \frac{2.5}{s} \tag{4.5}$$

The variation of equilibrium value of average thickness $\bar{H}$ is similar to that of L. It increases with h_e and for the same value of h_e, the it decreases with increasing slope.

A curve fit for the average thickness, as a function of L and s is as follows

$$\bar{H} = \frac{1}{1.4}\sqrt{\frac{L}{s}} \tag{4.6}$$

where L and H are expressed in metres. This fit is similar in form to the one used by Oerlemans (2008).

To check the usefulness of the curve fit, it is compared with observed values of thickness and length for a large number of glaciers from the World Glacier Inventory (WGI) database [http://nsidc.org/data/g01130.html]. One can see from figure 4.9, that the fit is within the range of observed values.

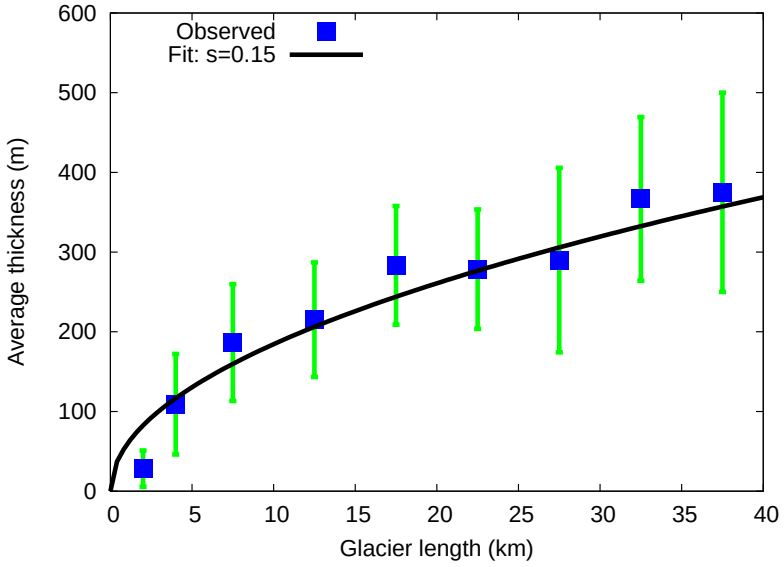

Figure 4.9: *Observed variation of mean thickness (filled squares), with error bars as function of L from WGI database. Solid line represents the curve fit for a value of s of 0.15.*

4.3 Application to real glaciers

As per our hypothesis,

$$\left.\frac{dL}{dt}\right|_{glacier} = \alpha F_1(L, H, s) + \frac{dh_e}{dt}\left(\frac{dL}{dh_e}\right) \tag{4.7}$$

This simplifies to

$$\left.\frac{dL}{dt}\right|_{glacier} = \alpha(sLH^{3/4}) + \frac{dh_e}{dt}\left(\frac{2.5}{s}\right) \tag{4.8}$$

where L is expressed in km and H is determined from equation 4.6.

Given the lengths, slopes and retreat rates of real glaciers, one can then find a least-squares, best-fit estimate of α and dh_e/dt. For a few glaciers, the control set, these quantities have been listed in table 4.2. Locations of these glaciers are given in figure 4.10. The retreat rates considered have been for the period of 25 years. The retreat rate for Khumbu is taken from Rai et al. (2005).

The best fit values are: $\alpha = 0.04053$ and $dh_e/dt = -0.6659$.

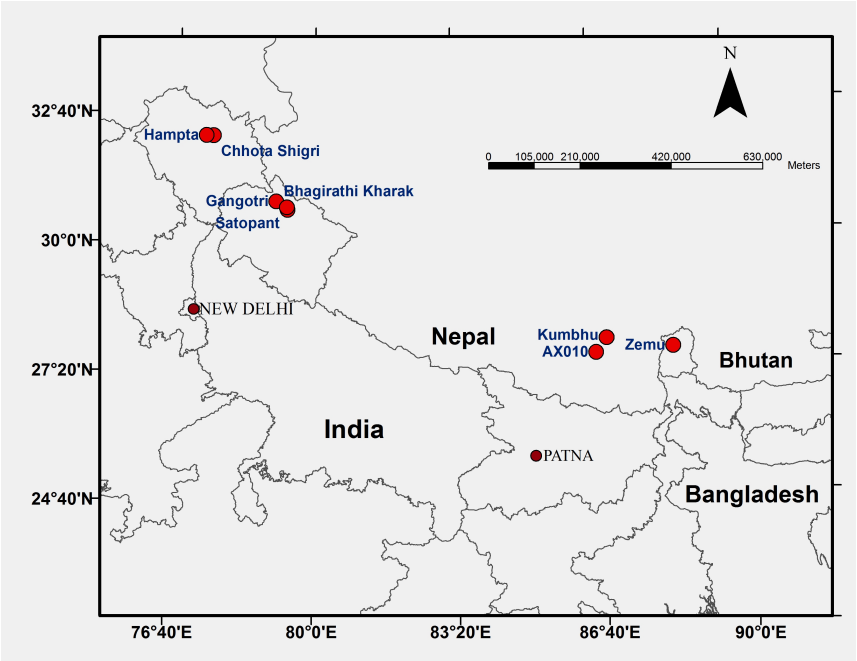

Figure 4.10: *Map showing the positions of the glaciers considered for the study.*

Glacier	Length (km)	Slope	Retreat (m/yr)	$F_1(L,s)$ (m/yr)	$\frac{dL}{dh}_e$
Hamtah	7.0	0.102	-16.00	24.64	24.51
Ch-Shigri	9.0	0.140	-7.17	46.17	17.86
Satopanth	14.0	0.150	-8.30	89.78	16.67
B-K	17.0	0.120	-7.30	96.89	20.83
Khumbu	17.5	0.176	-1.00	138.82	14.20

Table 4.2: *Length, slope, F_1 and dL/dh_e for the control set of glaciers.* [1]*: Ch-Shigri == Chhota Shigri and* [2]*: B-K == Bhagirath-Kharak.*

Using the values of α and dh_e/dt, the computed and observed values of retreat for the fitted set (glaciers listed in table 4.2) is shown in table 4.3 and the predicted set (AX010, Zemu and Gangotri) in table 4.4. The observed retreat rates are from Basnett et al. (2011) for Zemu and Kumar et al. (2008) for Gangotri.

4.4 Discussion

As one can see from tables 4.3 and 4.4, the computed values of retreat are close to what is observed. The RMS error for the first set is 1.61 m/yr and the second set is 3.82 m/yr. One should note that these values are comparable to the errors of measurement using field data. However, these differences are not significant, since our main aim is

Glacier	Length (km)	Slope	$\frac{dL}{dt}_{dyn}$ (m/yr)	$\frac{dL}{dt}_{thermo}$ (m/yr)	Retreat (obs) (m/yr)	Retreat (comp) (m/yr)
Hamtah	7.0	0.102	1.46	-16.32	-16.00	-14.86
Ch-Shigri	9.0	0.140	2.52	-11.89	-7.17	-9.37
Satopanth	14.0	0.150	4.83	-11.10	-8.30	-6.27
B-K	17.0	0.120	5.49	-13.87	-7.30	-8.38
Khumbu	17.5	0.176	7.26	-9.46	-1.00	-2.20

Table 4.3: *Computed and observed retreats for the fitted set. RMS error is 1.61 m/yr.*

Glacier	Length (km)	Slope	$\frac{dL}{dt}_{dyn}$ (m/yr)	$\frac{dL}{dt}_{thermo}$ (m/yr)	Retreat (obs) (m/yr)	Retreat (comp) (m/yr)
AX010	1.6	0.180	0.27	-9.25	-6.50	-8.98
ZEMU	28.0	0.135	11.74	-12.33	0.00	-0.59
GANGOTRI	30.0	0.076	9.01	-22.90	-19.00	-12.89

Table 4.4: *Computed and observed retreats for the predicted set. RMS error is 3.82 m/yr.*

to explain the balance between the two forces determining advance/retreat and not to match the exact value for any particular glacier. While the role of debris cover is not explicitly modelled, since the set of glaciers used for estimating the constants include glaciers with different amounts of debris cover, its effect is implicitly present.

For most of the glaciers, the dL/dt_{dyn} term is small and their behaviour is dominated by the climate term, leading to a net retreat. The relative roles played by the length and slope are brought out in Figure 4.11. In the first bar-chart, the glaciers are arranged in increasing order of slope. The retreat, is inversely proportional to slope. The tendency to advance depends on both the slope and length.

Although the lengths of Zemu and Gangotri glaciers are similar the rate of retreat is quite different. The Zemu glacier is almost stationary while the Gangotri glacier is retreating at the rate of 19 m per year. The proposed model suggests that the large difference in rate of retreat between these glaciers is on account of the difference in slope. The slope of Zemu glacier is almost double that of the Gangotri glacier. The higher slope of the Zemu glacier causes the advance due to gravity to be comparable to the ablation term leading to an almost zero rate of advance/retreat. The retreat of the Gangotri glacier is more sensitive to changes in mass balance because the slope of the glacier is much smaller. For the AX010 glacier, even though the slope is high, its short length, causes the advance term to be negligible and the climate term to dominate, leading to a net retreat.

The net retreat for both the sets is compared in figure 4.12, indicating a reasonably good match between the computed and observed values.

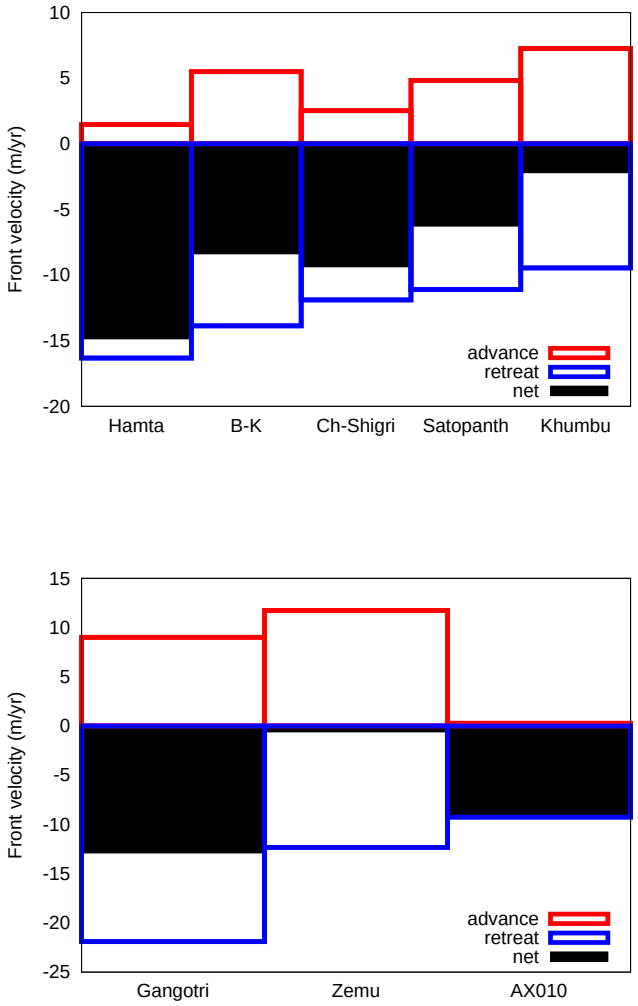

Figure 4.11: *Bar chart showing the balance of the opposing tendencies of advance due to dynamics (red boxes), retreat due to thermodynamics (blue boxes) and the net movement (black bars). The glaciers are arranged in increasing order of slope. Figures on the left are for the fitted set and those on the right are for the predicted set.*

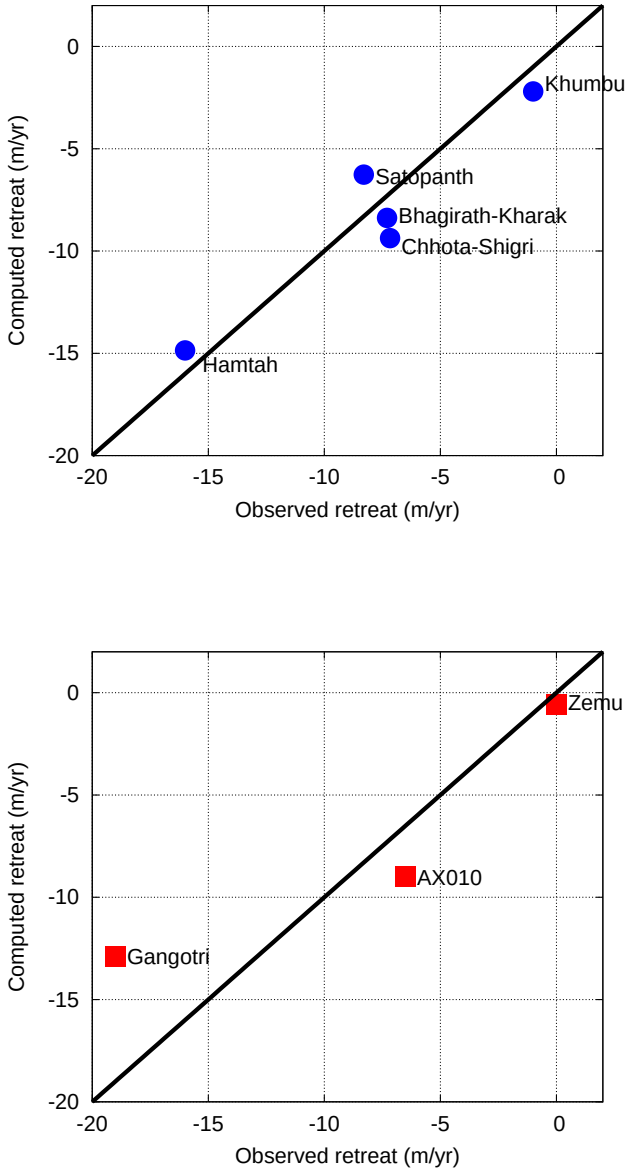

Figure 4.12: *Scatter-plot of observed retreat versus predicted retreat for the fitted set (left) and the predicted set (right).*

4.5 Application to larger datasets: Parbati and other basins

In the previous section, our model was applied to a small set of glaciers for which long term records of retreat are available. Application for a larger set is preferable to validate the model. However for larger sets which are available from satellites, the time period is less, which would not be appropriate for our model. Over a time period of 8 to 10 years, the inter-annual variations of snowfall/melting would dominate the observed retreat and the climate trends are not very clear. This is evident in the wide range of retreats from satellite data (maximum around 60 m/yr) than those from long term on-site observations (maximum around 20 m/yr). This has to be kept in mind while comparing these results.

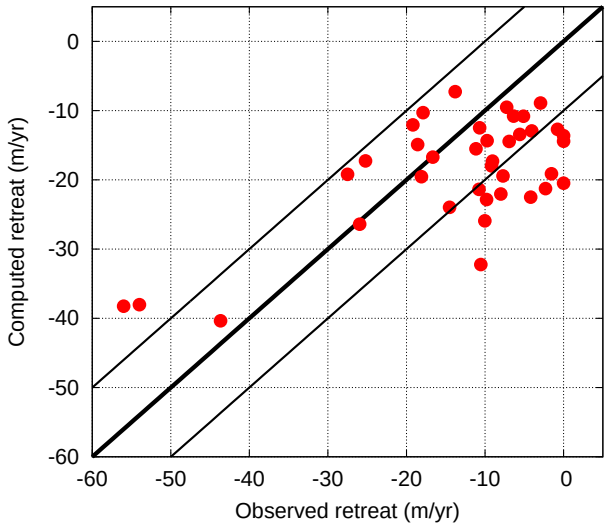

Figure 4.13: *Scatter-plot of observed retreat versus predicted retreat for the Parbati basin. The thinner lines represent the band of uncertainty (10 m/yr).*

First, we show the application to a larger set of 38 glaciers in the Parbati basin, for which retreat rates over a 11 year period are available. A subset of 15 glaciers was used to determine the coefficients in the model. The best fit values α and dh_e/dt were found to be 0.05 and -1.64 respectively. These coefficients were used to compute retreat rates for the complete set of 38 glaciers.

The scatter plot of observed versus computed retreat rates is shown in figure 4.13. One can see that the comparison is good for low values of retreat and reasonable for glaciers with high retreat (above 40 m/yr). There is scatter, is likely to be due to the shorter duration of data.

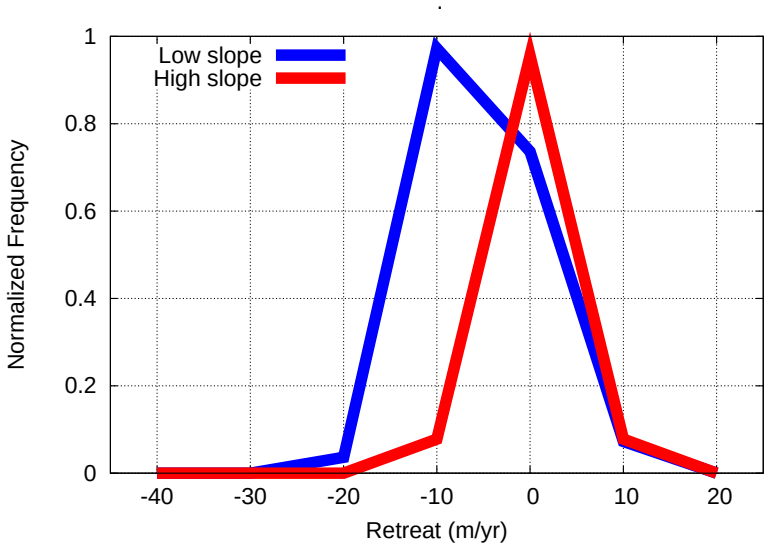

Figure 4.14: *Distribution of retreat rates for low slope (*0.14*) and high slope (*0.28*) for a simulated set of glaciers with length distribution similar to that of Scherler etal 2011.*

Now we apply the model to the set of glaciers of Scherler et al. (2011). Since the retreat rates are over a 8 year period, we do not compare for individual glaciers, but only the distribution. Distribution of retreat rates for a simulated set of glaciers, with length distribution similar to that of Scherler etal and slopes centered around two values: 0.14 (low slope) and 0.28 (high slope) is shown in figure 4.14. One can see that qualitatively, the distributions are similar to that for observed data (figure 4.3). In particular, the shift of 10 m/yr in the peak from low to high slopes is captures.

4.6 Summary

Using simulations with a numerical ice-flow model and simple hypotheses, we have demonstrated the relative effect of slope (dynamics) and equilibrium line altitude (thermodynamics) on the retreat of Himalayan glaciers. We have shown that the dynamics, as determined by the length and mean-slope can explain major differences in the behavior of glaciers when subject to the similar environmental changes. The decomposition of the glacier front velocity in terms of slope and ELA is a novel approach and as far as we know, quantification in these terms has not been done before.

The drastically different responses of Gangotri and Zemu, glaciers of nearly the same length, is explained well by this model. In the case of Zemu, the advance due to slope is around 11.7 m/yr which is balanced by retreat due to climate change, while for

Gangotri, the climate term dominates. Therefore, using only the observed retreat as an indicator of climate change, leads to erroneous conclusions.

The model has also been applied a larger set of glaciers in the Parbati basin, and other regions. For these glaciers, with retreat data over a shorter time-period, the distributions are well simulated.

While we have concentrated on mainly Himalayan glaciers, the concept is quite general and hence should be applicable to glaciers in other regions of the world.

Chapter 5

Application of simple model to other basins

The simple model to explain the relative role of slope and ELA was tested on the data of Scherler et al. (2011). Since the retreat rates are over a 8 year period, we do not expect the model to fare as well as for those glaciers with longer records.

The scatter plots for the individual basins are shown in figures 5.1, 5.2, 5.3, 5.4, 5.5 and 5.6. Only glaciers with low debris cover have been used.

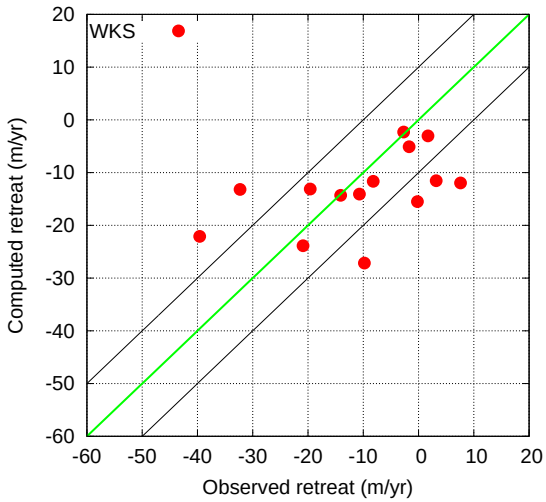

Figure 5.1: *Scatter-plot of observed retreat versus predicted retreat for the West Kunlun Shah basin.*

The model seems to work reasonably for WKS, WH and CHN basins, poorly for Karakoram and CHS basins. For the HK basin the number of glaciers with low debris

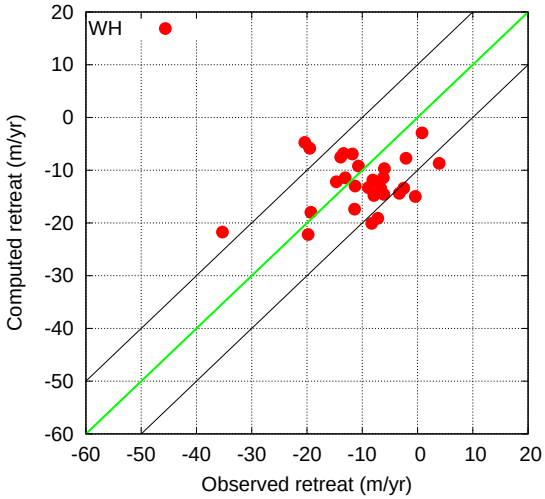

Figure 5.2: *Scatter-plot of observed retreat versus predicted retreat for the Western Himalyas basin.*

cover are small.

Grouping the basins into northern (WKS, K, HK) and southern (WH, CHS, CHN) sets, we see that the comparison is better for the northern set (figure 5.7) than the southern set (figure 5.8).

Other than the short span of the data, the reason why our simple model fits the observed retreats in some basins but not the others is not clear. This could be an interesting area for further research.

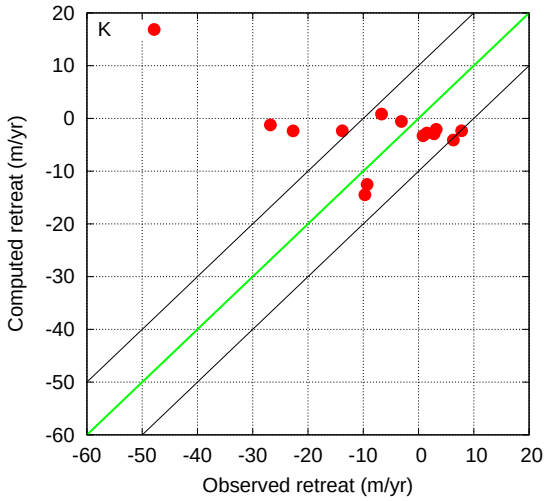

Figure 5.3: *Scatter-plot of observed retreat versus predicted retreat for the Karakoram basin.*

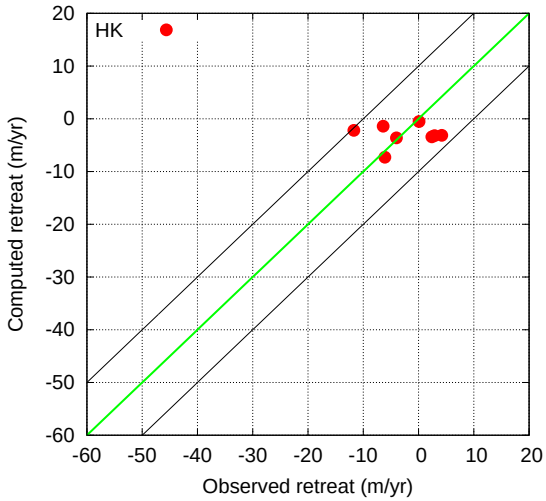

Figure 5.4: *Scatter-plot of observed retreat versus predicted retreat for the Hindu-Kush basin.*

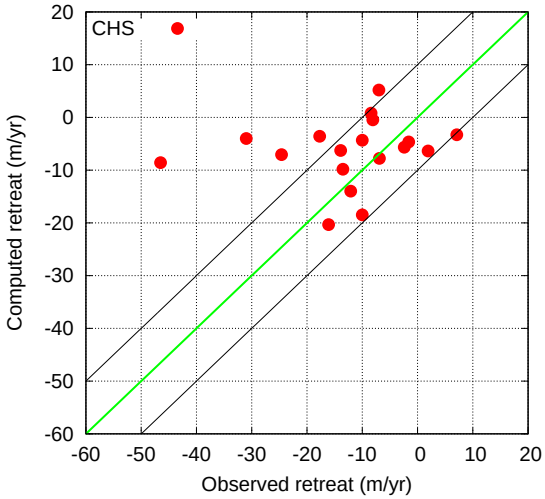

Figure 5.5: *Scatter-plot of observed retreat versus predicted retreat for the Central Himalayas South basin.*

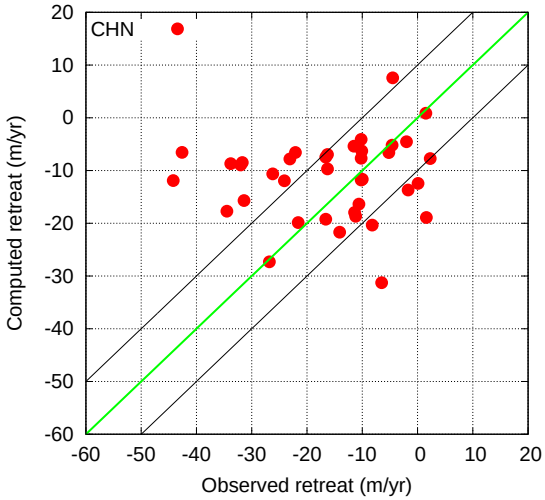

Figure 5.6: *Scatter-plot of observed retreat versus predicted retreat for the Central Himalayas North basin.*

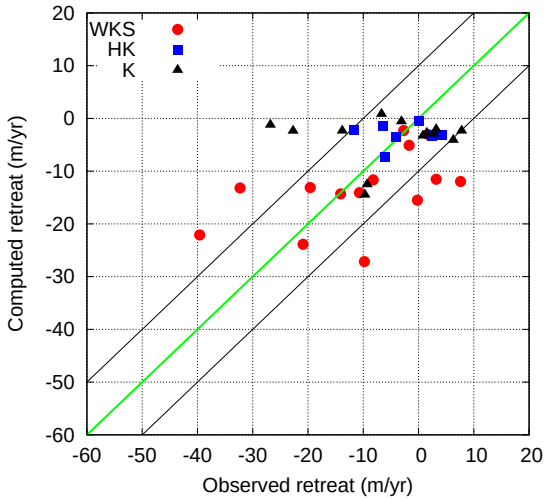

Figure 5.7: *Scatter-plot of observed retreat versus predicted retreat for the basins WKS, K and HK.*

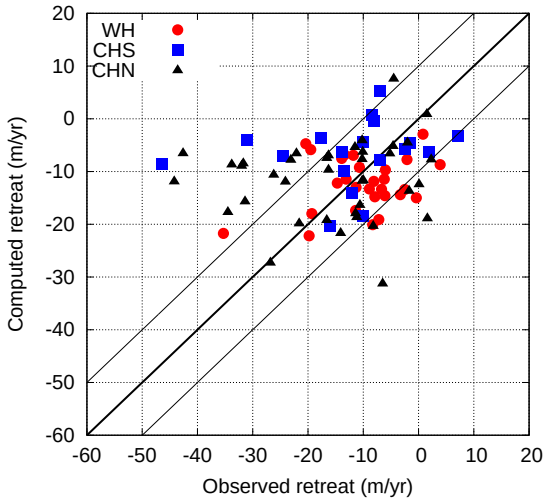

Figure 5.8: *Scatter-plot of observed retreat versus predicted retreat for the basins WH, CHS and CHN .*

Chapter 6

Climate projections

In this chapter some preliminary results of making prediction of future lengths of glaciers based on climate projections are described. The basis for these projections is the numerical ice-flow model. Since the main source term in the model is the mass-balance term, if the variation of this term is known as a function of time, the evolution of the glacier can be computed. In general, mass-balance is a function of the temperature and precipitation. This is the approach taken by (Adhikari and Huybrechts, 2009).

In climate simulations, there is more confidence in the temperature values than in the snowfall parametrizations. Observationally, also, no major tends in snowfall have been seen. Therefore, one could model mass-balance as a function of temperature alone. Temperature measurements at a glacier are rare. Usually, records at a nearby meteorological station are used. For Chhota-Shigri, temperature from the Patsio station, which is close is shown in figure 6.1. In addition, temperatures from other sources, such as IMD stations in Shimla and Manali and NCEP data are shown. The NCEP data (large-scale) does not show any significant trend. In the IMD station data at Manali and Shimla, a weak trend is visible. The observations in the Patsio station, which is closer in altitude to Chhota-Shigri, show a signifcant upward trend in temperature.

6.1 Observed mass-balance near Chhota-Shigri

Observed mass-balance data at the Chhota Shigri and also Hamtah glacier (which is nearby) is shown in figure 6.2.

A linear fit with temperature from the Patsio station is shown in figure 6.3. The following expression, where T is in degrees Celsius, has been used to relate the temperature to the mass balance.

$$B_m = -0.06(T - 1)$$

A difficulty here is that the mass-balances and temperatures are all not available for

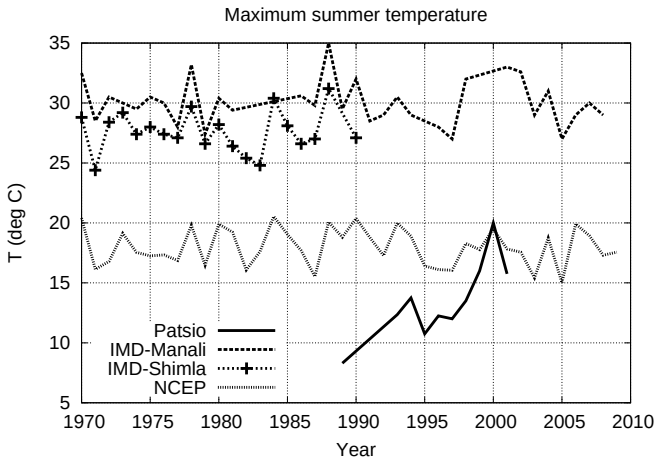

Figure 6.1: *Variation of temperature in the Himachal region from various sources.*

the same years.

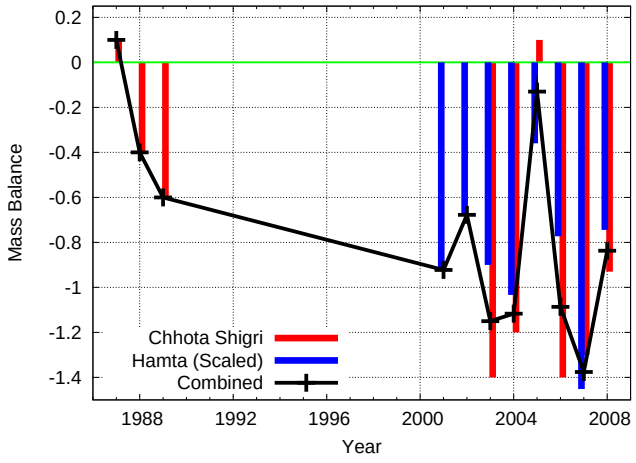

Figure 6.2: *Observed mass-balance data at the Chhota Shigri and Hamtah glaciers.*

6.1.1 Climate simulation

Rajendran and Kitoh (2008) used a very high resolution global general circulation model to study future climate change scenarios. The GCM, developed by JMA and MRI, Japan, was run at a spatial grid size of about 20 km and 60 vertical levels. T-959,

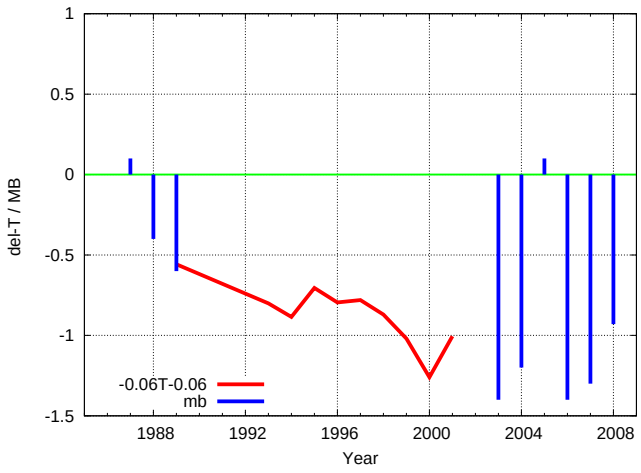

Figure 6.3: *Observed mass-balance and a fit using temperature at the Patsio station.*

1920x 960 grid. The IPCC A1B scenario was used for forcing.

Simulated temperature from the climate model of Rajendran and Kitoh (2008) at a grid-point close to the glacier Chhota Shigri. The altitude of the point in the model is 4573.47 m. Two sets of 25 year simulations were performed (figure 6.4).

In the intermediate region the temperature values were calculated so as to match the trend and main frequencies. This is shown in figure 6.5.

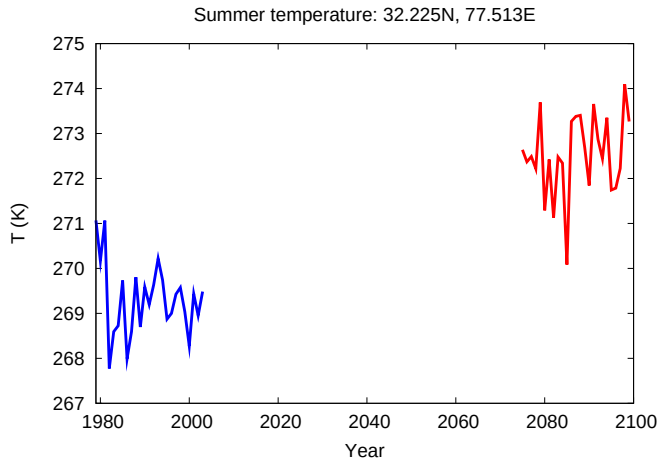

Figure 6.4: *Simulated temperature from the climate model at a grid-point close to the glacier Chhota Shigri. Two sets of 25 year simulations were performed.*

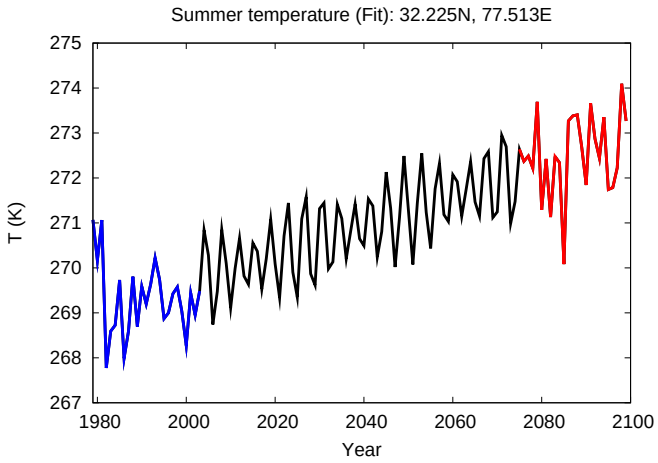

Figure 6.5: *Simulated temperature from the climate model interpolated in the intermediate region matching the trend and main frequencies.*

The inferred mass balance from the simulated temperature using a linear fit is shown in Figure 6.6. This mass balance was used for further integrations of Chhota-Shigri.

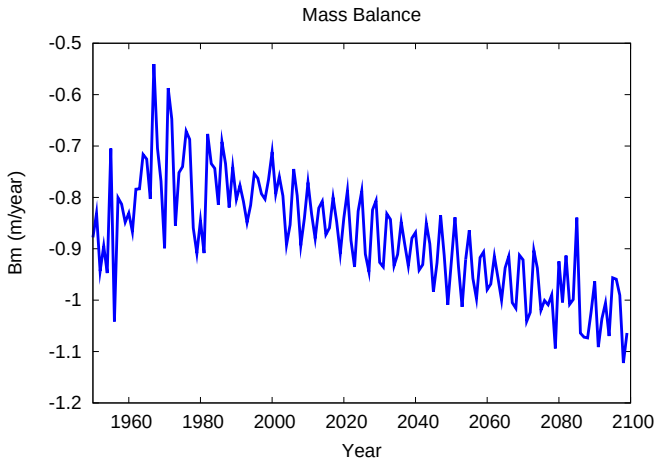

Figure 6.6: *Inferred mass balance from the simulated temperature using a linear fit.*

6.2 New integration strategy

Adhikari and Huybrechts (2009) have used observed mass-balance on a glacier and temperature data at a nearby meteorological station to find a relation and then used it for climate projections. For a smooth integration of the model, they also estimate past temperature and see that there is gradual transition. In this method they need a good estimate of the initial ice-thickness.

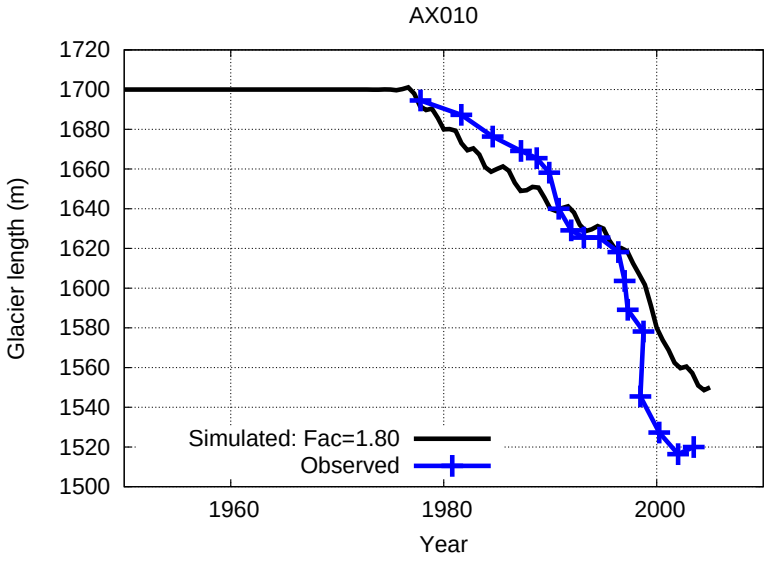

Figure 6.7: *Variation of the observed and simulated lengths for the glacier AX010.*

We have adopted a different approach: We start with zero ice-thickness and perform numerical integrations till a steady state is reached. The model parameters such as f_s and B_m0 are varied till the equilibrium length matches the observed length of the glacier and the rate of change matches the observed values. This configuration is then used for further integration. An advantage of this method is that ice-thickness distribution is not necessary as an input parameter. It is determined by the length which is observed. An example of this strategy is shown in figure 6.7.

6.3 Application to Chhota-Shigri

Computed evolution of the length of the Chhota-Shigri glacier in the recent past and projection up to 2100 are shown in figure 6.8.

The integration was started from 1960 using the new integration strategy. The factor multiplying f_s was varied to match the observed retreat upto latest available data (around 2005). Further integration was carried out using this factor and the mass balance estimated from projected temperature change.

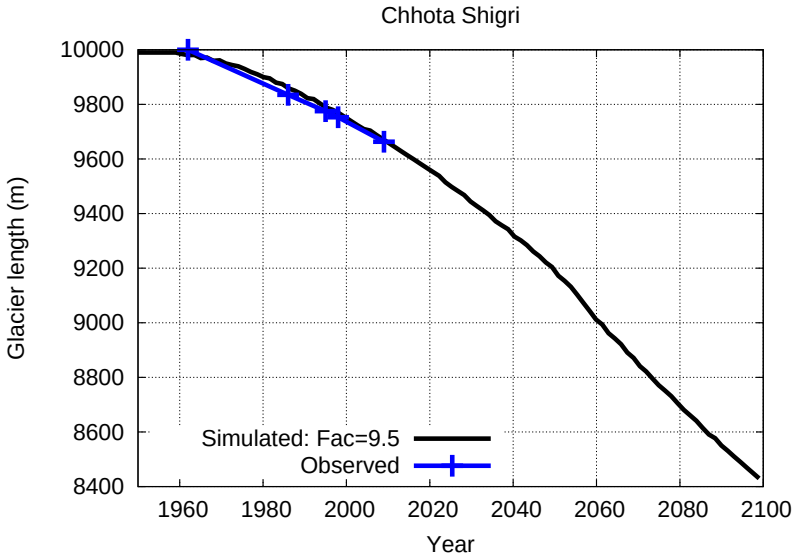

Figure 6.8: *Computed evolution of the length of Chhota-Shigri in the recent past and projection upto 2100.*

One can see that a retreat of around 1200 m is predicted upto 2100. This approach could be used for other glaciers as well and could be a topic for further research.

Chapter 7

Conclusion

We have studied the dynamics of glaciers using analytical and numerical models. We have developed a numerical ice-flow model based on the formulation of Adhikari and Huybrechts (2009) and used it to gain insight into the processes governing advance/retreat of glaciers.

We have proposed a simple model for estimating advance/retreat on a climate timescale, based on the slope and ELA and shown that the model works well for a number of glaciers with long-term records. In particular, the reason for the different behaviour of Gangotri and Zemu is explained by this model. The model has also been applied to larger datasets, for which it fares reasonably. These datasets are from satellite observations and have a shorter time-span.

Some analytical work to understand the behaviour of a simplified problem: a block of ice moving down an incline due to gravity, with ice-deformation, has been done. The closed-form solutions made possible with certain assumptions match qualitatively the numerical simulations and have provided insights into the behaviour.

In addition, some preliminary work towards, climate projections using the numerical ice-flow model has been done.

Bibliography

Adhikari, S.: Numerical modelling of historical front variations and the 21st century evolution of Glacier AX010, Nepal Himalaya", M. S. Thesis, Universiteit Gent Vrije Universiteit Brussel, Belgium, 2007.

Adhikari, S. and Huybrechts, P.: Numerical modelling of historical front variations and the 21st-century evolution of glacier AX010, Nepal Himalaya", Annals of Glaciology, 50 (52), 27 – 34, 2009.

Basnett, S., Kulkarni, A. V., Arrawatia, M. L. and Shrestha, D. G.: Glacier Studies in Sikkim Himalaya", Indian Institute of Science report no. IISC/DCCC/GLACIER/TR/001/2011 2011.

Benn, D. I., and Lehmkuhl, F.: Mass balance and equilibrium-line altitudes of glaciers in high mountain environments, Quaternary International, 65/66, 15 – 29, 2000.

Bolch, T., Yao, T., Kang, S., Buchroithner, M. F., Scherer, D., Maussion, F., Huintjes, E., and Schneider, C.: A glacier inventory for the western Nyainqentanglha Range and the Nam Co Basin, Tibet, and glacier changes 19762009, The Cryosphere, 4, 419–433, 2010.

Cuffey, K. M., and Patterson, W. S. B: The Physics of Glaciers, 3rd Edition, Butterworth-Heinemann, Elsevier, 2010.

Deota, B. S., Trivedi, Y. N., Kulkarni, A. V., Bahuguna, I. M. and Rathore B. P.: RS and GIS in mapping of geomorphic records and understanding the local controls of glacial retreat from the Baspa Valley, Himachal Pradesh, India", Current Science, 100 (10), 1555 – 1563, 2011.

Ganjoo, R. K. and Koul, M. N.: Is the Siachean glacier melting, Current Science 97(3), 309–310, 2009.

Kumar, K., Dumka, R. K., Miral, M. S., Satyal G. S. and Pant M.: Estimation of retreat rate of Gangotri glacier using rapid static and kinematic GPS survey, Current Science, 94(2), 258–262, 2008.

Kotlarski, S., Jacob, D., Podzun, R. and Paul, F.: Representing glaciers in a regional climate model, Climate Dynamics, 34:27 – 46 DOI 10.1007/s00382-009-0685-6, 2010.

Kulkarni, A. V., Rathore, B. P., Singh S. K., and Bahuguna I. M.: Understanding changes in Himalayan Cryosphere using remote sensing technique, International Journal of Remote Sensing 32(3), 601–615, 2011.

Kulkarni, A. V., Rathore B. P., Mahajan S., and Mathur P.: Alarming retreat of Parbati Glacier, Beas basin, Himachal Pradesh, Current Science 88(11), 1844–1850, 2005.

Kulkarni, A. V., Bahuguna, I. M., Rathore B. P., Singh, S. K., Randhawa, S. S., Sood, R. K. and Dhar, S.: Glacial retreat in Himalaya using Indian Remote Sensing satellite data, Current Science, 92(1), 69 – 74, 2007.

Nainwal, H. C., Negi, B. D. S., Chaudhary, M., Sajwan, K. S. and Gaurav, A.: Temporal changes in rate of recession: Evidences from Satopanth and Bhagirath Kharak glaciers, Uttarakhand, using Total Station Survey, Current Science, 94(5), 653 – 660, 2008.

Oerlemans, J.: Simulation of historic glacier variations with a simple climate-glacier model, Journal of Glaciology, 34, 118, 333–341, 1988.

Oerlemans, J.: Extracting a climate signal from 169 glacier records, Science, 308, 675 – 677, 2005.

Oerlemans, J.: Minimal Glacial Models, Igitur, Utrecht Publishing & Archiving Services, Universiteitsbibliotheek Utrecht, 2008.

Polyanin A. D. and Zaitsev V. F. (2003)
"Handbook of non-linear Partial Differential Equations"
Chapman and Hall, CRC, 2003

Rai, S. C. editor: An Overview of Glaciers, Glacier Retreat, and Subsequent Impacts in Nepal, India and China, WWF Nepal Program report, 2005.

Rajendran K and Kitoh A
Indian summer monsoon in future climate projection by a super high-resolution global model. *Current Science*, 95, 1560 – 1569, 2008.

Scherler, D., Bookhagen, B., and Strecker, M. R.: Spatially variable response of Himalayan glaciers to climate change affected by debris cover, Nature geoscience, PUBLISHED ONLINE: 23 JANUARY 2011 — DOI: 10.1038/NGEO1068, 2011

Siddiqui, M. A., Maruthi, K. V., Nayak S. K., and Hampaiah, P.: Detailed glaciological studies on Hamtah glacier, Lahaul and Spiti district, Himachal Pradesh, Publication of Geological Survey of India, F.S. 2004-05 GL/NR/HQ/1999/001, 2005.

Swaroop, S., and Shukla, S. P.: Report on glacier front fluctuation studies in parts of H. P. and U. P., Publication of Geological Survey of India, 1999.

WGI database URL: http://nsidc.org/data/g01130.html

Yong, N., Yili, Z., Linshan, L., Jiping, Z., Glacial change in the vicinity of Mt. Qomolangma (Everest), central high Himalayas since 1976, J. Geogr. Sci., 20(5), 667-686, 2010.

Appendix A

One-D icemodel: Source code

```
!-----------------------------------------------------------------------
!     Simple Glacier Model
!-----------------------------------------------------------------------
!     Written by : T. N. Venkatesh
!                  tnv@flosolver.nal.res.in
!-----------------------------------------------------------------------
!     Based on
!
!     Adhikari & Huybechts, 2009, Annals of Glaciology, 50(52), 27 - 34
!     Adhikari Thesis, 2007
!-----------------------------------------------------------------------
!     Equation being solved
!
!     d H         1   d ( w U H )
!     ---    +   --  -------------       =    B (x,t)
!     d t         w   d  x
!
!     Where
!             x       : direction along flow-line
!             H(x, t) : height of the ice at station x
!             w(x)    : width of the ice at station x
!             U(x, t) : Velocity at station x
!             B(x, t) : Mass balance at station x
!-----------------------------------------------------------------------
!-----------------------------------------------------------------------
      program glacmo
!.....Declarations
      integer, parameter :: MAX_X = 5000
      integer, parameter :: MAX_T = 10000
```

```
      integer            :: n_x,n_t,  i,j
      integer            :: iyr_start, iyr_end
      integer            :: ispin, ispin_start, ispin_end
      real               :: delta_t, del_x
      real               :: rho_ice, f_s, f_d, scale_fac
      real               :: f_s0, f_d0,  Equi_Line_Alt

      character*256      :: w_filename, bm_filename,elev_filename
      character*256      :: ice_filename, out_filename

      real,dimension(MAX_X) :: H_ice_n, H_ice_np1, H_ref, U_ice
      real,dimension(MAX_X) :: rate_H, rate_H_0, H_temp
      real,dimension(MAX_X) :: w_glac, elev_glac, B_mass_grid

      integer,dimension(MAX_T)  ::  iyear
      real,dimension(MAX_T)     ::  B_mass_hist
!.....Start
      write(*,*) "Simple glacier model"

      rho_ice = 850.0    ! kg/m^3

!.....Read config file
      open(unit=11,file='glac.inp',status='old',iostat=ifile_ok)
      if (ifile_ok /= 0 ) then
        write(*,*)
        write(*,*) " ERROR opening file: glac.inp"
        stop
      endif

      read(11,*)
      read(11,*) n_x,n_t
      read(11,*)
      read(11,*) iyr_start, iyr_end, delta_t
      read(11,*)
      read(11,*) ispin,  ispin_start, ispin_end, bm_spin
      read(11,*)
      read(11,*) f_s0, f_d0, scale_fac
      read(11,*)
      read(11,*) Equi_Line_Alt, del_x
      read(11,*)
      read(11,*) w_filename, bm_filename,elev_filename
      read(11,*)
      read(11,*) ice_filename
      read(11,*)
      read(11,*) out_filename
```

```
      close(unit=11)

      f_s = f_s0 / scale_fac
      f_d = f_d0 / scale_fac

      open(unit=12,file=out_filename,status='unknown',iostat=ifile_ok)
      if (ifile_ok /= 0 ) then
        write(*,*)
        write(*,*) " ERROR opening file:", out_filename
        stop
      endif
      write(12,*) "#-----------------------------------------------"
      write(12,*) "# ", "n_x           =",n_x
      write(12,*) "# ", "n_t           =",n_t
      write(12,*) "# ", "iyr_start     =",iyr_start
      write(12,*) "# ", "iyr_end       =",iyr_end
      write(12,*) "# ", "ispin         =",ispin
      write(12,*) "# ", "ispin_start   =",ispin_start
      write(12,*) "# ", "ispin_end     =",ispin_end
      write(12,*) "# ", "bm_spin       =",bm_spin
      write(12,*) "# ", "f_s0          =",f_s0
      write(12,*) "# ", "f_d0          =",f_d0
      write(12,*) "# ", "scale_fac     =",scale_fac
      write(12,*) "# ", "ELA           =",Equi_Line_Alt
      write(12,*) "# ", "w_filename    :  ", TRIM(w_filename)
      write(12,*) "# ", "elev_filename :  ", TRIM(elev_filename)
      write(12,*) "# ", "ice_filename  :  ", TRIM(ice_filename)
      write(12,*) "# ", "bm_filename   :  ", TRIM(bm_filename)
      write(12,*) "#-----------------------------------------------"


!.....Read input files
      call read_arr(n_x, w_filename,     w_glac)
      call read_arr(n_x, elev_filename,  elev_glac)
      call read_arr(n_x, ice_filename,   H_ref)

      call read_arr(n_t, bm_filename,  B_mass_hist)


!.....Initialize
      if (ispin.eq.1) then
        do j = 1, n_x
          H_ice_n(j) = 0.0
```

```
          H_ice_np1(j) = H_ice_n(j)
        enddo
      else
        do j = 1, n_x
          H_ice_n(j) = H_ref(j)

          H_ice_np1(j) = H_ice_n(j)
        enddo
      endif

      nsteps = 1.0/delta_t + 0.5
      write(*,*) "nsteps = ", nsteps

!-----------------------------------------------------------------------
!.....Main integration loop
!.......Loop over years
        do iyr = iyr_start, iyr_end

          jspin = 0
          if ((iyr.ge.ispin_start).and.(iyr.le.ispin_end))  then
            jspin = 1
          endif

!.........Calc. mass balance rate for this year
          do i = 1, n_x
            H_top = elev_glac(i) + H_ice_n(i)
            if (jspin.eq.1) then
            B_mass_grid(i) = 0.01*(H_top - Equi_Line_Alt)
     &                       + bm_spin
            else
            B_mass_grid(i) = 0.01*(H_top - Equi_Line_Alt)
     &                       + B_mass_hist(iyr-ispin_end+1)
            endif
          enddo

!.........Time integration loop: within a year
          do n = 1, nsteps

            do i = 1, n_x
             H_ice_n(i) = H_ice_np1(i)
            enddo
!...........Calculate rates
            call calc_rate_H(H_ice_n, B_mass_grid,
     &                       w_glac, elev_glac,  del_x,
     &                       n_x, f_s,  f_d, rho_ice,
```

```
!
     &                        U_ice, rate_H_0)
            do i = 1, n_x
              H_ice_np1(i) = H_ice_n(i) + delta_t* rate_H_0(i)
            enddo

            do i = 1, n_x
              if (H_ice_np1(i).lt.EPS) then
                H_ice_np1(i) = 0.0
              endif
            enddo
          enddo ! END of loop within a year
          call find_max(n_x, U_ice, U_max)
          call find_max(n_x, H_ice_np1, H_max)

          ig_length = 0
          do i = 1, n_x
           if (H_ice_np1(i) .gt. EPS) then
             ig_length =  ig_length + 1
           endif
          enddo
          write(12,*) iyr,  ig_length*del_x, H_max, U_max
          write(*,*)  iyr, ig_length*del_x, H_max, U_max

        enddo ! END of loop over years
!-----------------------------------------------------------------------
!.....End of Main integration loop

!.....Store results / analysis
      rewind(30)

      do i = 1, n_x
        write(30,*) i*del_x, H_ice_np1(i), elev_glac(i)
      enddo
      close(unit=12)

      stop
      end
!-----------------------------------------------------------------------
      subroutine read_arr(n_a,  a_filename,  var_a)
      character*256  a_filename
      real, dimension(n_a) :: var_a

      open(unit=11,file=a_filename,status='old',iostat=ifile_ok)
      if (ifile_ok /= 0 ) then
```

```
        write(*,*)
        write(*,*) " ERROR opening file:", a_filename
        stop
      endif

      read(11,*)
      do i = 1, n_a
        read(11,*) var_a(i)
      enddo
      close(unit=11)


      return
      end
!-----------------------------------------------------------------------
      subroutine calc_rate_H(H_ice, B_mass,
     &                         w_glac, elev_glac,  del_x,
     &                         n_x, f_s,  f_d, rho_ice,
     &                       U_ice, rate_H)

      integer              :: n_x

      real, parameter      :: gee = 9.81         ! m / s^2
      real, dimension(n_x) :: H_ice, B_mass, w_glac, elev_glac
      real, dimension(n_x) :: U_ice, rate_H
      real                 :: f_s,  f_d, rho_ice,  del_x

!.....Local variables
      real, dimension(n_x) :: diff_H

      EPS = 1.0e-8

!.....Calculate effective diffusivities
      do i = 2, n_x
        H_av = H_ice(i)
        dhdx = -( (elev_glac(i+1)+H_ice(i+1))  -
     &            (elev_glac(i-1)+H_ice(i-1))  )/(2.0*del_x)
!.......D
        rhogh_cube = (rho_ice*gee*H_av)**3
        w_av = w_glac(i) + H_ice(i)
        diff_H(i) =  w_av*rhogh_cube *(dhdx**2)*(f_s+f_d*H_av*H_av)
!.......Deformation velocity
        S_d = rho_ice * gee * H_av * dhdx
        S_d_cube  = S_d**3
        U_d = f_d * S_d_cube * H_av
```

```
!.......Sliding velocity
        if (H_av.gt.EPS) then
          U_s = (f_s * S_d_cube) / H_av
        else
          U_s = 0.0
        endif

        U_ice(i) =  U_d + U_s
!        write(*,*) i, H_av, dhdx, S_d_cube, U_d, U_s
      enddo

      U_ice(1)    = 0.0
      diff_H(1)   = 0.0
      diff_H(n_x) = 0.0

!      U_ice(n_x) = 0.0

!.....Calculate rates
      do i = 2, n_x-1
        w_t = w_glac(i) + 2.0*H_ice(i)
        w_a = w_glac(i) + H_ice(i)

        D_p = 0.5*(diff_H(i) + diff_H(i+1))
        D_m = 0.5*(diff_H(i) + diff_H(i-1))
        dhdx_p =  ( (elev_glac(i+1)+H_ice(i+1)) -
     &                     (elev_glac(i  )  +H_ice(i))) / del_x
        dhdx_m =  ( (elev_glac(i  )+H_ice(i  )) -
     &                     (elev_glac(i-1)+H_ice(i-1))) / del_x

!.......AH-form
        HUw_p = D_p * dhdx_p
        HUw_m = D_m * dhdx_m

        d_HUw_dx  = (HUw_p - HUw_m)/ del_x
        if ( w_t .gt. EPS) then
          advec_term =  d_HUw_dx/w_t
        endif
        rate_H(i) =    B_mass(i) + advec_term
      enddo
      rate_H(1)   =  0.0
      rate_H(n_x) =  0.0

      return
      end
!-----------------------------------------------------------------------
```

```
      subroutine  find_max(n_x, var_a, var_max)

      real, dimension(n_x) :: var_a

      var_max = var_a(1)
      do i = 2, n_x
        if (var_a(i).gt.var_max)  then
          var_max = var_a(i)
        endif
      enddo

      return
      end
!-----------------------------------------------------------------------
```

Appendix B

Parameters used for a typical run

```
#-----------------------------------------------
# n_x           =         298
# n_t           =         408
# iyr_start     =        1200
# iyr_end       =        2005
# ispin         =           1
# ispin_start   =        1200
# ispin_end     =        1600
# bm_spin       =  0.3200000
# f_s0          =  1.8000000E-12
# f_d0          =  6.0000002E-17
# scale_fac     =   3.250000
# ELA           =   5210.000
# w_filename    :  width-ax100.dat
# elev_filename :  elev0.dat
# ice_filename  :  icebase-ax100-01.dat
# bm_filename   :  mb-comb.dat
#-----------------------------------------------
```

Appendix C

Sample glacier geometry data

```
################################
#  Chhota Shigri:  Geometry
################################
#  x      h_b      h_t       w_t
# (m)     (m)      (m)        (m)
#-------------------------------
-1000    5200     5200       218.62
 -861    5125     5150       655.86
 -615    5050     5100      1005.65
 -246    4975     5050       918.20
#-------------------------------
    0    4900     5000      1093.10
  280    4800     4950      1399.17
  700    4750     4900      1311.72
  840    4750     4900      1355.44
 1120    4800     4880      1355.44
 1670    4700     4825      1093.10
 2050    4700     4780       874.48
 2420    4600     4750       874.48
 2740    4600     4725      1049.38
 3160    4575     4700      1093.10
 3490    4600     4675      1136.82
 4000    4500     4650      1093.10
 4420    4525     4625       874.48
 4840    4500     4575       743.31
 5020    4475     4550       655.86
 5390    4450     4500       612.14
 5950    4400     4450       568.41
 6320    4350     4390       524.69
 6560    4330     4350       480.96
```

```
 6700    4300     4325       480.96
 7440    4175     4190       306.07
 8000    4050     4050       131.17
#--------------------------------
 8100    4025     4025       100.0
 8200    4007     4007       100.0
 8300    3994     3994       100.0
 8400    3979     3979       100.0
 8500    3963     3963       100.0
 8600    3949     3949       100.0
 8700    3937     3937       100.0
 8800    3924     3924       100.0
 8900    3912     3912       100.0
 9000    3900     3900       100.0
 9100    3890     3890       100.0
 9200    3881     3881       100.0
 9300    3875     3875       100.0
 9400    3867     3867       100.0
 9500    3859     3859       100.0
 9600    3851     3851       100.0
 9700    3842     3842       100.0
 9800    3834     3834       100.0
 9900    3824     3824       100.0
10000    3813     3813       100.0
10100    3798     3798       100.0
10200    3780     3780       100.0
10300    3762     3762       100.0
10400    3743     3743       100.0
10500    3717     3717       100.0
10600    3694     3694       100.0
10700    3670     3670       100.0
10800    3636     3636       100.0
10900    3600     3600       100.0
11000    3548     3548       100.0
11100    3500     3500       100.0
#--------------------------------
```

REPORT IISc-DCCC 12 CC1
JUNE 2012

DIVECHA CENTRE FOR CLIMATE CHANGE
INDIAN INSTITUTE OF SCIENCE
Bangalore